Progress In Electromagnetics Research B, Vol. 80, 173–198, 2018

An Overview of UWB Antennas for Microwave Imaging Systems for Cancer Detection Purposes

Berenice Borja[1, *], Jose A. Tirado[1], and Hildeberto Jardón[2]

Abstract—In the last decades, microwave imaging has been a new area of research due to its many advantages over current imaging systems. Microwave imaging system is used for in-depth inspection of biological tissues. The test provides the identification of morphological changes in these biological tissues, as well as their locations. The emerging Ultra-Wideband (UWB) microwave imaging gives better result with the main advantage of using non-ionizing radiation. In these systems, antennas play a very important role, and as such, their optimization has become a very important topic because the device is placed close to the human body. Thus, many aspects are of great importance in the design of the antennas starting from the material with which it is constructed, its dimensions, operation bandwidth, human body influence on the antenna parameters, short-pulse propagation, etc. Recent research has shown several efforts in improving the electromagnetic sensors used in these systems, either as individual or array elements. In this paper, we provide an overview of the most relevant developments in the field of UWB high directivity sensors used in microwave imaging systems.

1. INTRODUCTION

Human body cells divide themselves to keep their integrity and to work properly. If this division process is modified, a tumor or nodule is formed. If the latter invades some other nearby biological tissues, it will become a malignant tumor, better known as metastasis, which derives in cancer [1].

Healthy biological tissues and abnormal ones differ morphologically from each other, and this difference is a direct consequence from both cell total water content variation and property changes of the membrane cell. It has been demonstrated that the biological tissues possess conductive properties, and its electrical resistivity is calculated as a function of frequency [2]. Thus, with the previous considerations, it is possible to calculate a dielectric scatter factor to identify cancer wounds [2].

Cancer is an asymptomatic disease, which means that in early stages the patient has no warning signs or pain until the disease reaches an advanced stage. Hence, it is ideal to achieve cancer detection in early stages in order to increase the chances to get a successful oncologic treatment. Most clinical imaging tests are currently based on the interaction of electromagnetic or acoustic waves with body tissues and fluids [3], but not all of them operate in the same frequency range. Regardless of the different types of clinical imaging tests, X-ray is used more as it provides more reliable diagnostic. X-rays are radiations of high-energy electromagnetic waves, and although ionizing radiation has been shown to have several beneficial applications for humans, it can also produce detrimental effects [4] even when X-rays are a diagnosis test [5]. The interaction of radiation with cells is a function of probability, i.e., there may or may not be interaction, and if the interaction occurs, damage may or may not occur [6]. Thus, its use on biological tests increases the probability to produce permanent changes in the cells which will trigger cell mutation until its death as shown in Figure 1 [7].

Received 3 March 2018, Accepted 9 May 2018, Scheduled 27 May 2018
* Corresponding author: Berenice Borja (bborjab0900@alumno.ipn.mx).
[1] Department of Electrical Engineering, ESIME-IPN, Mexico City, Mexico. [2] Department of Electrical Engineering, CINVESTAV-IPN, Mexico City, Mexico.

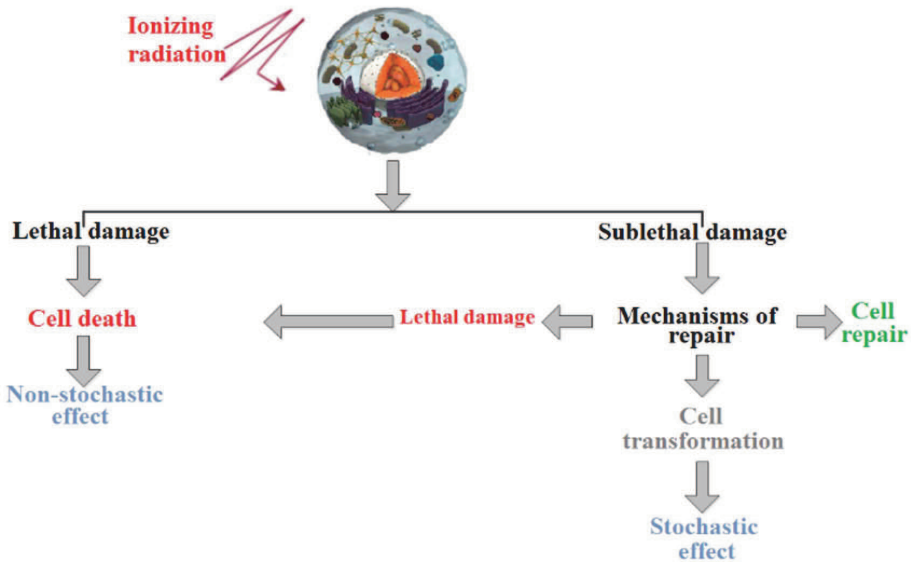

Figure 1. Damage to DNA by ionizing radiation [7].

Due to the reasons mentioned above, in recent years, many efforts have been dedicated to find a reliable cancer diagnostic tool avoiding the use of ionization energy. In that sense, some techniques based on microwave signals using image reconstruction algorithms have been investigated [8–11]. Compared to X-rays, microwave imaging can be safely repeated more frequently because it is free from ionizing radiation [12].

2. RADIOFREQUENCY AS A CANCER DIAGNOSTIC TOOL

The use of microwaves in the medical field has generated several applications, one of them as a diagnostic tool. Radiofrequency can be used to create medical images based on the contrast between the dielectric properties of healthy and malignant tissues [13], due to the interaction of electromagnetic waves with matter. The interaction of electromagnetic waves and matter depends on dielectric properties which can be directly related to various types of biological constituents due to their varying degree of water content: bone, fat, muscle, etc. [14]. Imaging systems that employ microwave radar techniques are a promising tool due to the high contrast obtained between normal tissue and tumors [11], non-ionizing, low-cost system, reduced safety concerns, potential to detect small tumors [15] and may be a tool suitable for frequent screening [16].

The use of electromagnetic energy in the microwave frequency range is particularly attractive because it balances the competing requirements for resolution and penetration depth [17, 18]. Likewise, these requirements, the image resolution and the depth penetration on biology tissues are directly related to the antenna used in the system. Both concepts are critical cancer diagnostic tests as they define the quality of the contrast between a tumor and nearby biological healthy tissue, as well as the detection efficiency of a mass or nodule.

From several studies [11, 18, 19], it is concluded that an excellent compromise between high-range resolution images and deep penetration into biological tissue can be reached through the use of either a single directive UWB antenna or an antenna array configuration [18]. The latter is possible since, within the range from 1 GHz to 10 GHz [13], the electromagnetic waves are capable to penetrate biological tissue in a very efficient way and maintain a reasonable attenuation [11], because at higher frequencies beyond 10 GHz waves can exhibit scatter effects on the skin surface [19].

Thus, it is promising to get an early stage cancer detection test by an electrical characterization of biological tissues. These diagnosis systems will get data from highly directive microwave sensors, which are basically designed to detect the changes on permittivity of the biological tissues, to be processed by imaging reconstruction techniques. The permittivity is normally high at lower frequencies due to an

insulating effect of cell membranes and decreases over higher frequencies due to scattering [14].

One of the most important elements in microwave imaging system is the antenna, which will receive or transmit electromagnetic energy. One of the main challenges in the design of these antennas is related to the physical size in order to allow a greater number of antennas to collect more information of the scattered signal for a successful image reconstruction, as well as to achieve a wider bandwidth to get a high-resolution image [20] and reduce the distortion in transmission of short-duration pulses [21]. Several antennas were proposed for cancer detection as monopole antennas [14, 22], fractal antennas [23–26], antipodal Vivaldi antennas [27], slot antenna [28, 29], and patch antenna [30], as will be described below.

3. UWB ANTENNAS IN MICROWAVE IMAGING SYSTEMS

Many of the imaging diagnostic tools are focused on breast cancer detection, due to the high rate of cases. This method usually uses antenna arrays of poor directivity and performs over a fractional bandwidth between 70% and 85%. Furthermore, a compact, low-profile antenna design is additionally desirable to reduce the complexities of the physical array structure and to achieve a degree of conformality with the body. Different types of antennas are considered in tissue-sensing applications using pulsed radar techniques such as: resistively loaded bowtie, slot line bowtie, ridged pyramidal horn, resistively loaded dipole and microstrip Archimedean spiral [31].

The above-mentioned systems had their beginnings on analyzing the dielectric properties of breast carcinoma and the surrounding tissues [13], and the measurements revealed significant differences in dielectric properties, which can be associated with the cellular heterogeneity and structural differences of the tissues [13]. In [32], Benjamin et al. studied a 2D ground penetrating radar (GPR) system for microwave detection of buried mines, so that in 2003 Nilavalan et al. [33] performed the same analysis on biological tissues. Analogous to GPR, microwaves are transmitted employing model antenna array as shown in Figure 2(a). The antenna array model consists of 16 microstrip-fed wideband stacked patch antenna elements [34] as those presented in Figure 2(b). The results obtained in [16] and [33] derived using backscatter data, from an anatomically realistic 2D-FDTD model, demonstrate successful detection of a small tumor (2 mm-diameter) in a lossy-inhomogeneous human breast [16].

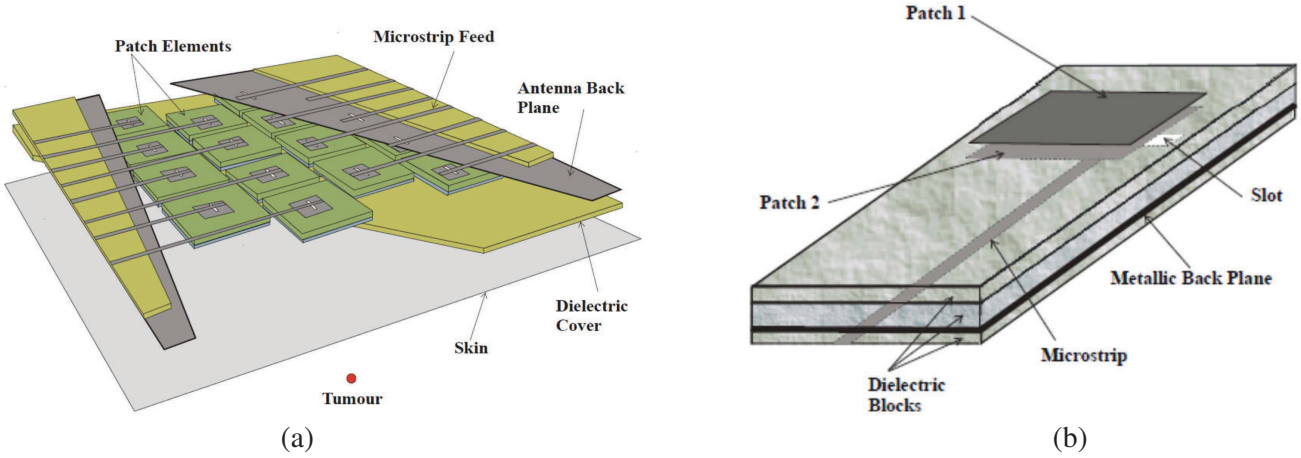

Figure 2. FDTD model: (a) 16 microstrip-fed wideband stacked patch antenna elements [16] and (b) stacked patch antenna [34].

In 2004, these theoretical results were confirmed by means of a mechanical-scan with only two-antennas [34] and a synthetic biological material (gelling agent and water). The stacked patch antenna presented in [34] operates between 4.5 and 9.5 GHz, and radiates into a medium with a dielectric permittivity of 9.5 (emulsion of oil and water). However, the scanner was limited in accuracy and scan-time, thus, it was decided to replace it with a 16-elements stacked-patch antenna array as shown in Figure 3(a). This array follows the design model presented in [16], where the antennas were printed on a $\varepsilon_r = 2.2$ dielectric substrate which was separated from the antenna ground plane with a $\varepsilon_r = 10.2$

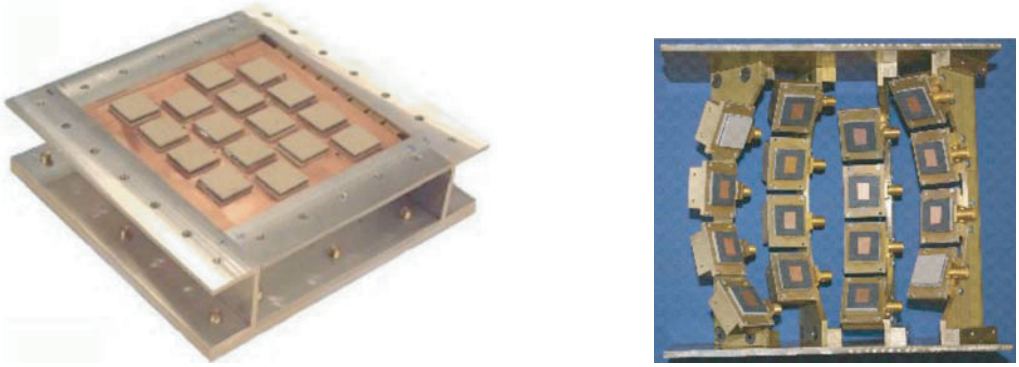

(a) (b)

Figure 3. UWB antennas array for microwave imaging systems for breast cancer detection: (a) planar stacked-patch 16-antennas array [35] and (b) semispherical conformal 16-antennas array [36].

substrate [35]. The results show that synthetic tumors (4 and 15 mm size) are detected at their correct locations, especially that the 15 mm tumor is detected in the presence of skin clutter; however, the 4 mm tumor needed a full subtraction background [35]. The skin-reflection is a significant obstacle to detecting smaller tumors.

Planar stacked-patch 16-antenna array shown in Figure 3(a) will assist in the development of a curved-array clinical prototype since it is difficult to have the breast in uniform contact with such a structure. In this hemispherical conformal 16-antenna array [36], each element is positioned tangentially to the spherical surface as can be seen in Figure 3(b).

The main difference between the two arrays is that the elements of the first one was printed on the same substrate, while in the second one, the elements are manufactured on separate substrates and fed by a coaxial line. In addition, each antenna is cavity-backed to eliminate undesired back-reflections and to reduce the effects of the surrounding environment. To achieve this goal absorbent material is used as shown in Figure 4

(a) (b)

Figure 4. Cavity backed aperture stacked patch antenna for breast imaging: (a) front side [37] and (b) back side [37].

In 2007, Klemm et al. optimized a symmetrically curved antenna array, and at the same time, the realistic 3D curved breast phantom with appropriate electrical properties is used [38]. Unlike the earlier prototype shown in Figure 3(b), in the symmetrically curved antenna array (second-generation), the antennas were aligned in rows and columns, and the array has two axes of symmetry as shown in Figure 5(a). This optimization is possible due to the size reduction of the sensor of approximately by 50% [39]. The reduction was made on the substrate/ground-plane cross-section size without considerable changes in its performance. With the contribution of Craddock et al. in [39], Klemm et al. optimized the design to an initial clinical prototype developed at the University of Bristol [40] as shown in Figure 5(b).

Clinical trials started with actual breast cancer patients at the Bristol Oncology Center. The tests were based on the comparison of a mammogram of a woman with breast cancer and a corresponding image using the developed radar-based microwave system [40]. The microwave system has, apparently,

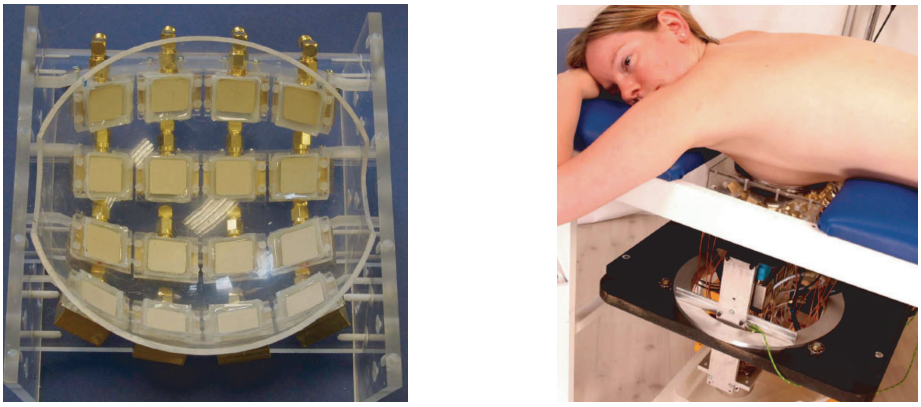

(a) (b)

Figure 5. Microwave radar-based clinical setup for breast cancer detection: (a) photograph top view of symmetrical curved antenna array [38] and (b) photo of the initial clinical prototype setup with a patient [40].

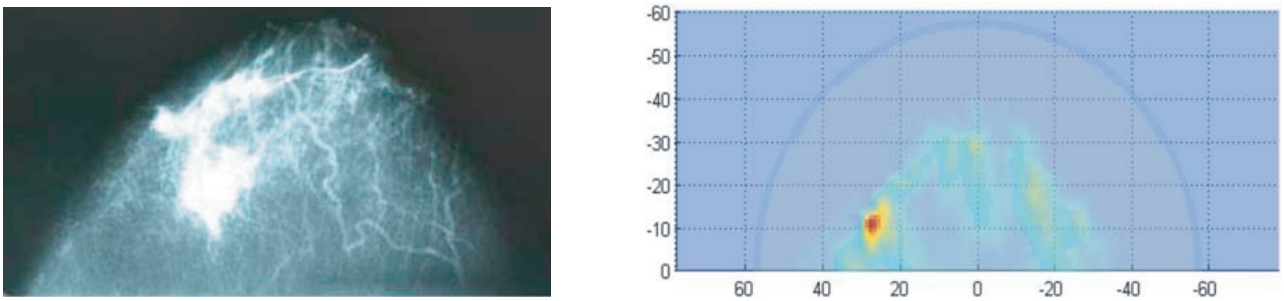

(a) (b)

Figure 6. Comparison of the clinical imaging results: (a) X-ray mammogram [40] and (b) 2D radar based UWB microwave system [40].

successfully detected the tumor in correct position when the two images are compared as shown in Figure 6, although compression of the breast during mammography makes it impossible to determine an exact position of the tumor [40].

Regardless of the adopted image method, the properties of the antenna play a fundamental role, and because of this, some research groups have been interested in the optimization of antennas used in these systems. The initial work at Bristol [31] only focused on developing a low-profile and wideband antenna, and as a result the antenna used was presented in Figure 2. However, imaging systems such as that presented in Figure 5 are limited by clutter, and hence, in these multi-static arrays there is a significant advantage in increasing the number of sensors [41]. In this specific case, the array area cannot be increased because it should be near the shape of the breast. That is why the elements must be reduced so that the array, with the same area, contains more sensors. This will allow more information to be gathered which, in turn, will reduce clutter in the result. Gibbins et al. [41] proposed to optimize the microstrip-line-fed printed wide-slot antenna of Sze and Wong [42]. The smaller antenna size, as seen in Figure 7, facilitates the increment of the number of elements in the array.

Figure 8(a) shows the difference in size between the antennas presented in Figure 4 and Figure 7. Both antennas were designed to work with a cavity. In addition, the feed for the last antenna has been modified to eliminate the SMA connector, further reducing the overall dimensions as shown in Figure 8(a). As a result of this size reduction of the antenna, in [43, 44] a new 31-cavity backed UWB wide-slot element array is presented, distributed around the available hemispherical surface as shown in Figure 8(b).

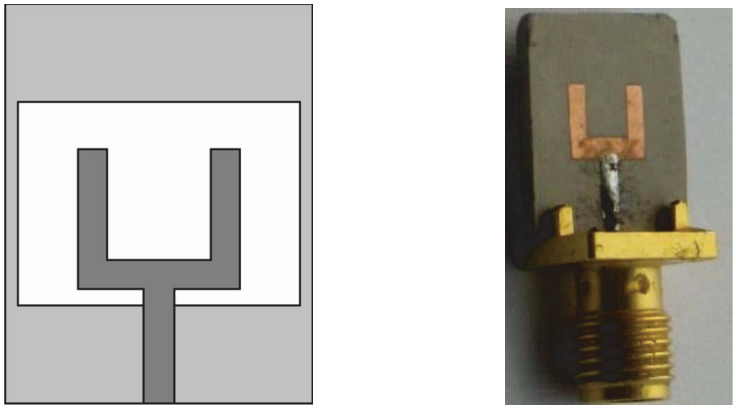

(a) (b)

Figure 7. Microstrip-line-fed printed wide-slot antenna: (a) schematic [41] and (b) the manufactured antenna [41].

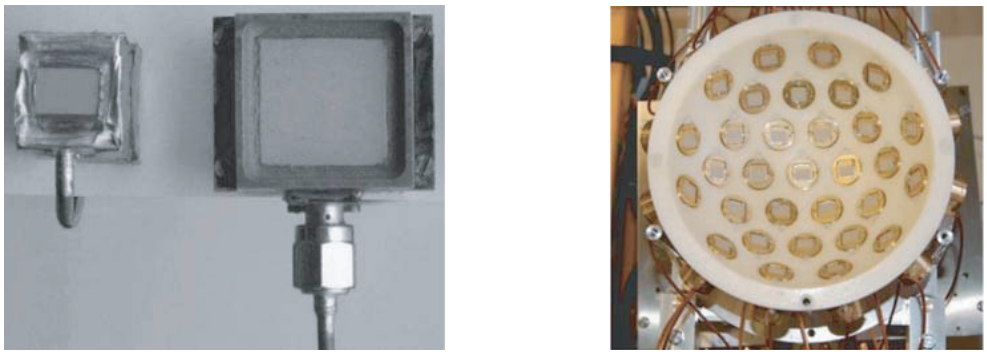

(a) (b)

Figure 8. New element for novel microwave radar-based imaging system: (a) comparison of the wide-slot antenna fed directly from a coaxial cable (left) and the SMA fed stacked patch antenna (right) both with a prototype cavity [29] and (b) complete 31-element hemispherical array [44].

A clinical trial was undertaken at the Breast Care Centre of Frenchay Hospital [40]. In this scenario, imaging in a clinical environment is quite different from that using a laboratory phantom; as a result, some problems were presented with the patients such as difficulties of fitting a wide range of breast sizes to the curved array, movement during scan (breathing during the scan) and tissue properties (breast interior is more complex than assumed with the phantoms). However, repeatability in phantoms was excellent. In other words, the conclusion was, therefore, that slight patient movement during the scan time was the major factor [45]. Another problem that arises in the system is that when the tumors are large, they tend to be detected as several distinct masses rather than a single one [44]. The scan time used in the system presented in Figure 8(b) was approximately 90 seconds, considered as a large range of scan time, because this is the period where the patient starts moving, thus it is desired to decrease scan times [45].

With the aim of decreasing scan times, full wave electromagnetic solvers were used to optimize the position of 60 slot elements around a hemispherical section (only a few mm larger than the first design) as shown in Figure 9. The new system provides 1770 measurements in just 10 seconds, therefore accomplishing the original objective of a dramatic improvement in speed [45].

In New Hampshire, US, the Dartmouth Hitchcock Medical Center (academic medical center) uses the 3-D system microwave tomographic images shown in Figure 10. The system consists of 16 monopole antennas organized in a circular array, and each antenna sequentially transmits an electromagnetic wave

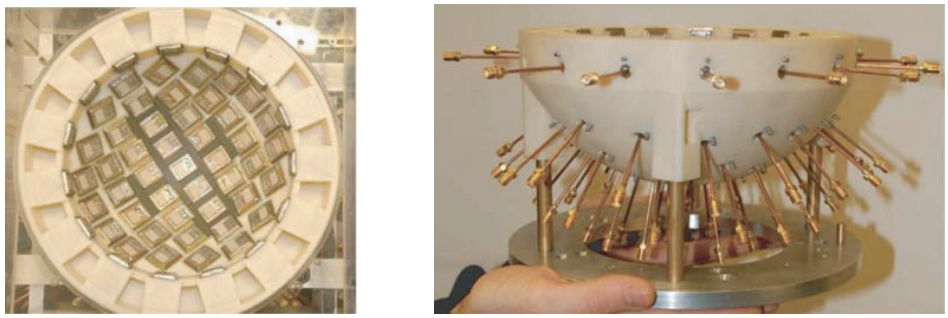

(a) (b)

Figure 9. New 60-element antenna array: (a) plan view [45] and (b) side view [45].

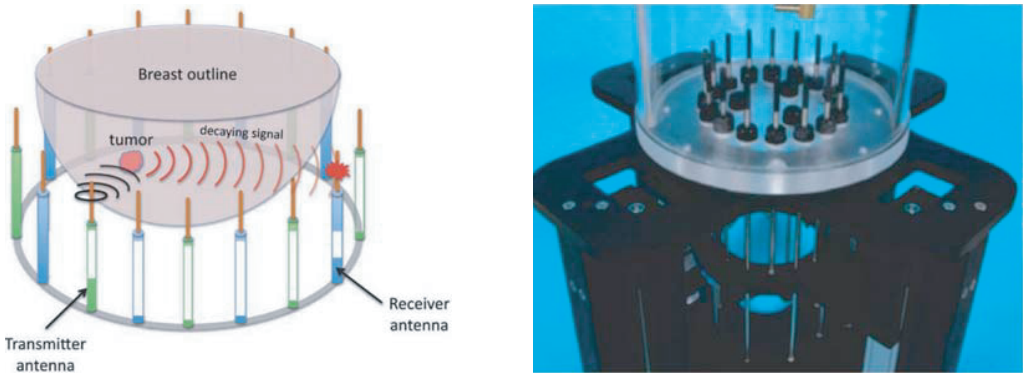

(a) (b)

Figure 10. Data acquisition platform for breast cancer detection: (a) schematic 3-D representation [14] and (b) photograph of system of tomographic microwave imaging setup [14].

which propagates through the breast within the imaging region. Measurements are collected at the remaining 15 antennas so that those close to the radiator mainly measure waves reflected from tissue surfaces whereas those opposite to the transmitter mainly measure transmitted waves. The multi-view scattered intensity and phase distributions provide information about the local dielectric properties of the transilluminated tissues [14].

The antennas are simple monopoles which, when being submerged in a lossy liquid, provide the necessary radiation characteristics: omnidirectional pattern for full target coverage and good broadband, impedance matching [14]. Grzegorczyk et al. [14] state that their technology presents important advantages that could complement other imaging modalities: it is safe (low power level), fast (data acquisition is less than 2 min, and image processing is currently under 20 min), low cost, does not require reagents, and is noninvasive. Ref. [14] specifies that in order to achieve sub-centimeter resolution, operating frequency of 1.3 GHz is often optimal, although this depends somehow on breast composition.

A similar array to those presented above can be observed in Figure 11. The hemispherical array consists of 16 compact bowtie antennas, in which the feeding network and bowtie were constructed on different substrates. The radar-based setup operates in the frequency range of 1.2 up to 7 GHz, thereby improving the penetration of the EM waves in the breast. The radiator was printed on a substrate of low permittivity, while that for the feeding network of each element was printed on a substrate of high permittivity [46].

In this type of arrays, the antennas make contact with the breast or are very close to it, which means that some areas of illumination are affected, or there is no biocompatibility. In Figures 12(a) and (b), single and dual polarized planarized monopole antennas can be observed, which solve these limitations. The elements are printed on a kapton substrate using the ink-jet technology making them

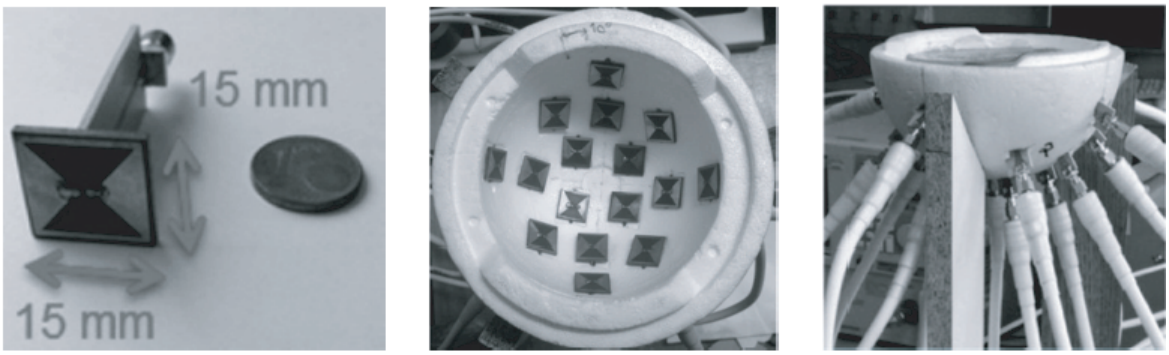

(a) (b) (c)

Figure 11. Compact near-field imaging system for breast cancer detection: (a) bowtie antenna perspective view [46], (b) array configuration on a styropor base top view [46] and (c) side view [46].

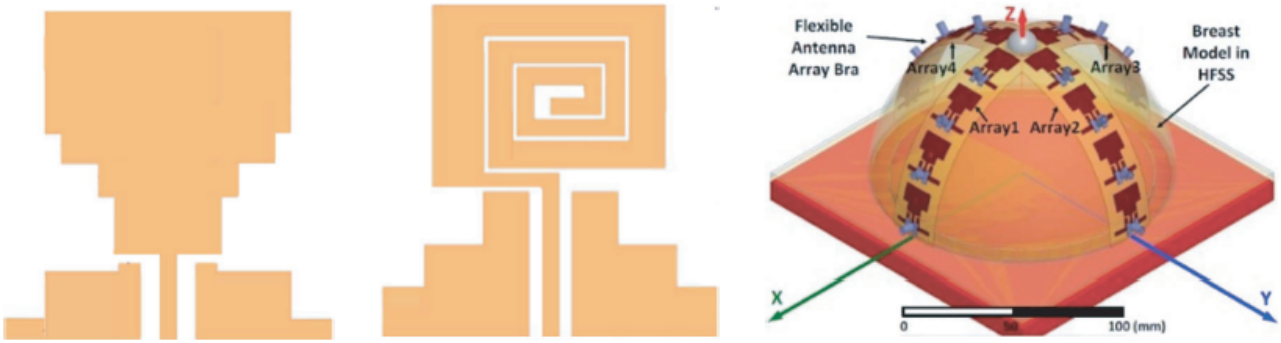

(a) (b) (c)

Figure 12. Flexible antenna array for breast cancer detection: (a) flexible monopole antenna [22], (b) flexible single-arm spiral antenna [22] and (c) flexible monopole 16-antennas array side view [22].

discrete, flexible, biocompatible and smooth as shown in Figure 12(c). This kind of substrate allows the elements to take the shape of the breast, maintaining adequate coverage over the area under study between 2 and 5 GHz. Adding reflectors behind the array improves the power gain and the ability to detect the presence of tumor [47].

The mentioned findings were the basis for the design shown on Figure 13. The 16 elements array was mounted on a bra using kapton as a substrate, and this is considered as an innovative, comfortable and portable design, and therefore more profitable, achieving a better quality of the acquired data and the position of the breast tissue with respect to the array [48].

Using the same type of dielectric material as in [48], Wang and Arslan [49] present a Co-Planar Waveguide (CPW)-fed UWB antenna on a DuPont Kapton substrate with fractal patterns as can be seen in Figure 14. Nowadays, there has been an expanding quantity of literature of fractal UWB antennas [23–26, 50, 51]. The antenna shown in Figure 14 covers from 2.5 GHz to 6.5 GHz frequency range, and fractal slots on the radiator increase the gain compared to using full printed radiators achieving a gain of 5 dB at 6 GHz. The antenna is printed on a 75 μm thickness substrate ($36 \times 26\,\text{mm}^2$) and is suitable for wearing on the human body for imaging application [49]. The kapton polyimide film substrate provides a good balance of physical, chemical, and electrical properties [52]; however, other performance alike substrates exist such as electro-textile, paper-based, fluidic, and synthesized flexible substrates [53].

Katbay et al. [51] designed a Hilbert fractal antenna for the use in Industrial, Scientific and Medical (ISM) band (2.45 GHz) where the signal attenuation in human body is quite small. The antenna is printed on a Plexiglas substrate ($\varepsilon_r = 3.6$) with total dimensions of $13.5 \times 32.4\,\text{mm}^2$ [50]. As in previous

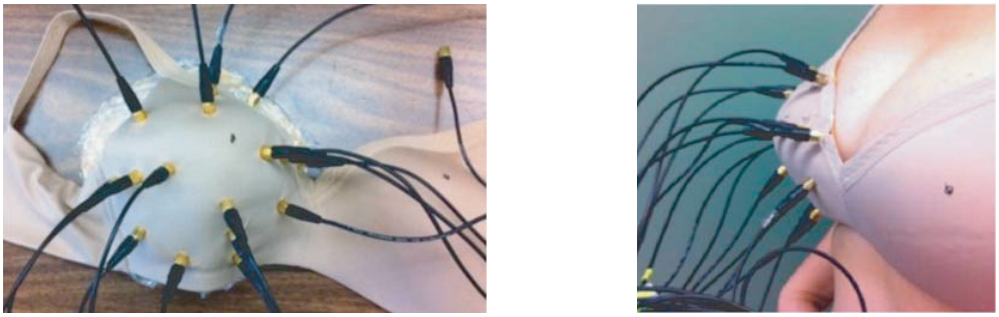

(a) (b)

Figure 13. The wearable prototype: (a) photograph of the outside of the bra showing the SMA cables that connect to the antennas (the bra is sitting on a breast model) [48] and (b) fitted to a volunteer with cables [48].

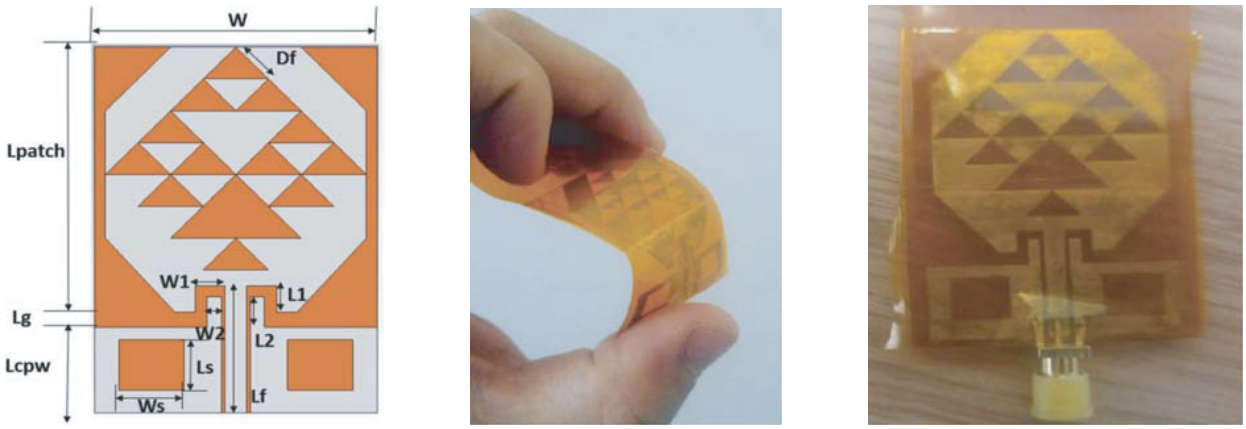

(a) (b) (c)

Figure 14. CPW-fed UWB antenna: (a) geometry [49], (b) inkjet-printed flexible antenna [49], and (c) assembly with SMA connector [49].

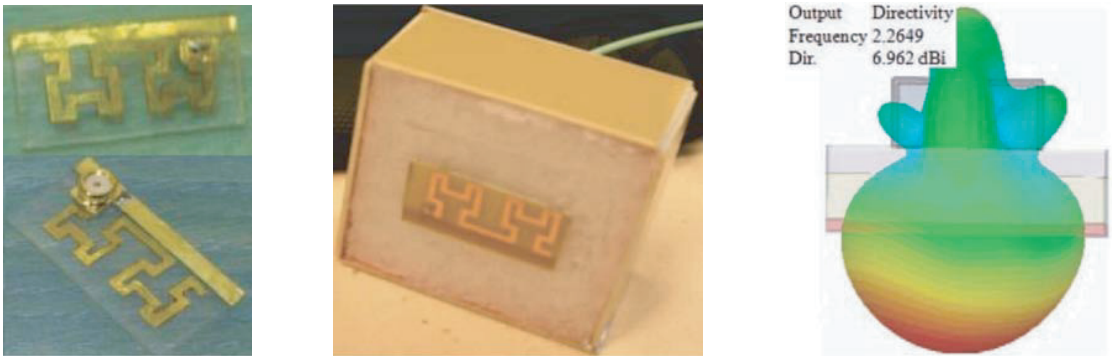

(a) (b) (c)

Figure 15. Miniature Hilbert fractal antenna: (a) fabricated antenna [50], (b) back-cavity [51], and (c) radiation pattern with the back-cavity at 2.26 GHz [51].

designs, when the designed antenna is positioned in direct contact on the skin, the resonance frequency is down-shifted, the antennas radiation pattern deformed, and the gain and directivity are decreased due to the interaction antenna-body. This interaction antenna-body causes that an important part of the incident wave is back-reflected because the tissue is a lossy medium with a high permittivity compared

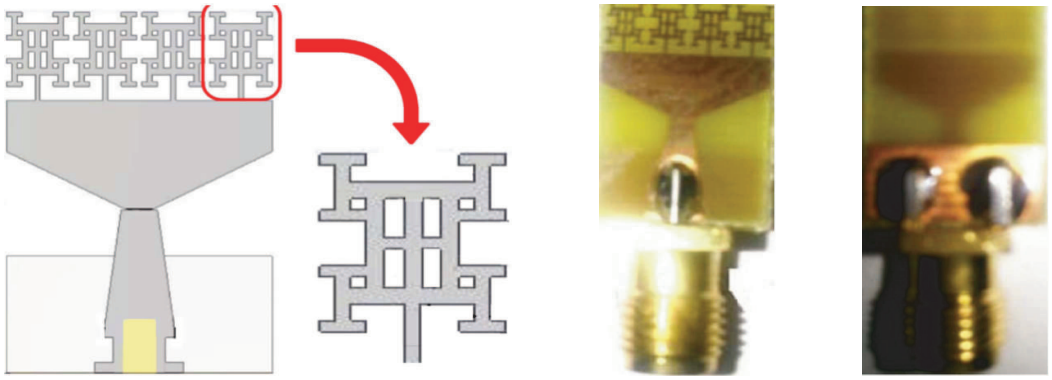

(a) (b) (c)

Figure 16. Compact UWB monopole antenna with four identical unit cells: (a) geometry [20], (b) fabricated front antenna [20], and (c) fabricated back antenna [20].

to the air. In order to minimize the radiation outside the human body, the antenna is placed inside a rectangular cavity to increase the antenna directivity and to focalize the energy in the phantom as shown in Figure 15(b). The directivity of the antenna is globally enhanced about 3 dB at 2.2 GHz.

In [20] a very compact UWB monopole antenna for breast cancer detection was designed by Afifi et al., and the main differences of this antenna compared to others are its size and radiating patch that has four identical unit cells as shown in Figure 16(a). The function of the unit cells is basically that the effective area of the unit cell structure is large due to longer path followed by the signal along the unit cell boarders, and the field radiated at the corners will greatly reduce the amount of energy that reflects at the truncation of the structure [20]. The proposed UWB antenna has bandwidth about 10 GHz, ideal for providing a good resolution for microwave imaging, and gain of approximately 3 dB up to 10 GHz [20].

There are other prototypes with slightly better characteristics such as gains and bandwidths, but they use fractal techniques [23–26]. However, the dimensions are increased considerably compared to the one presented by Afifi et al. ($10 \times 10\,\text{mm}^2$) [20], and the performance of this UWB antenna is dependent on the fractal patch, feeding, slots on the partial ground plane achieving approximately gains of 4 dB, and omnidirectional radiation patterns. Figure 17 shows different antennas with fractal techniques.

Similar to [20], in [30] four left-handed metamaterial (LHM) unit cells are located along one axis of the antenna as the radiating element. The antenna has a partial ground plane containing a rectangular slot on the upper portion as shown in Figure 18. The metamaterial unit cells are inserted on the

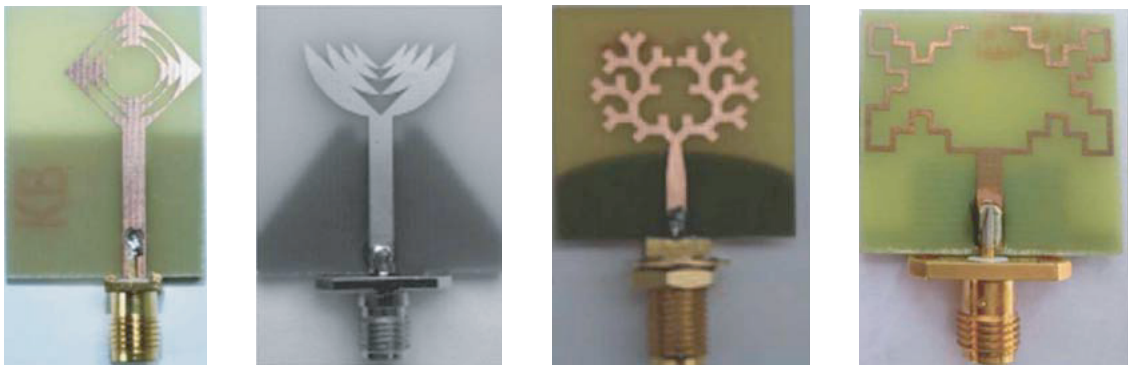

(a) (b) (c) (d)

Figure 17. UWB fractal antennas: (a) 4th iteration [23], (b) 4th iteration [24], (c) 3rd iteration [25], and (d) Minkowski-like geometry [26].

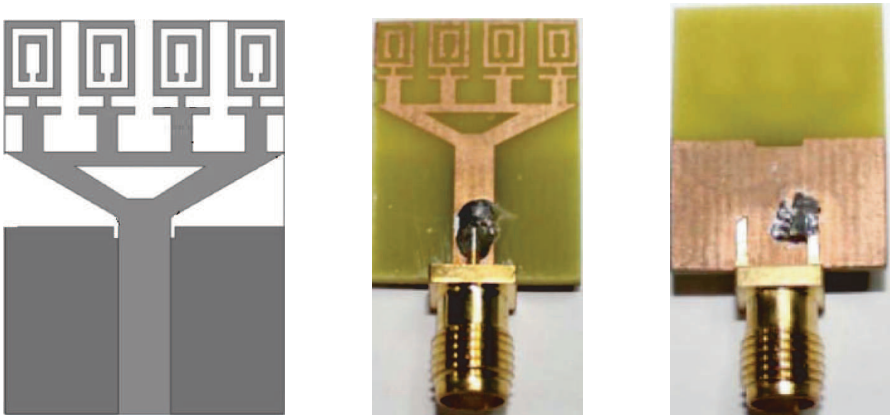

(a) (b) (c)

Figure 18. A negative index metamaterial antenna for UWB microwave imaging applications: (a) geometry layout [30], (b) fabricated front antenna [30], and (c) fabricated back antenna [30].

radiating patch with a modified split-ring resonator (SRR) and capacitively loaded strips (CLS) to show both negative permittivity and negative permeability, which assures the stable negative refractive index to raise the antenna performance for microwave imaging [30]. The antenna has a total dimension of $16 \times 21\,\text{mm}^2$, gain of approximately 5 dB at 10 GHz, and omnidirectional radiation patterns [30]. An LHM structure is also used to increase the gain of the microstrip antenna by placing the LHM structure in front of the patch antenna. As a result, the gain increases approximately 4 dB, but this technique also makes physical size of the antenna increased [54].

Another way to improve the directivity in monopole antennas without modifying the design of the radiator patch is adding a simple reflector as shown in Figure 19(a). Latif et al. [56] present an elliptical monopole antenna with high-permittivity material; however, using this type of material reduces the size of the antenna, which leads to reducing the bandwidth and limiting the gain. For radar-based imaging applications an antenna with UWB and high gain performance is required for high-resolution image reconstruction, thus, a reflector under antenna is used to cause high coupling of power to the tissue, although this considerably increases the overall dimensions of the antenna [56]. In the same way, High Impedance Surface (HIS) has been introduced like reflectors to improve antennas profile [57, 58]. These reflectors allow realizing low profile antennas and improve radiation patterns while preserving their

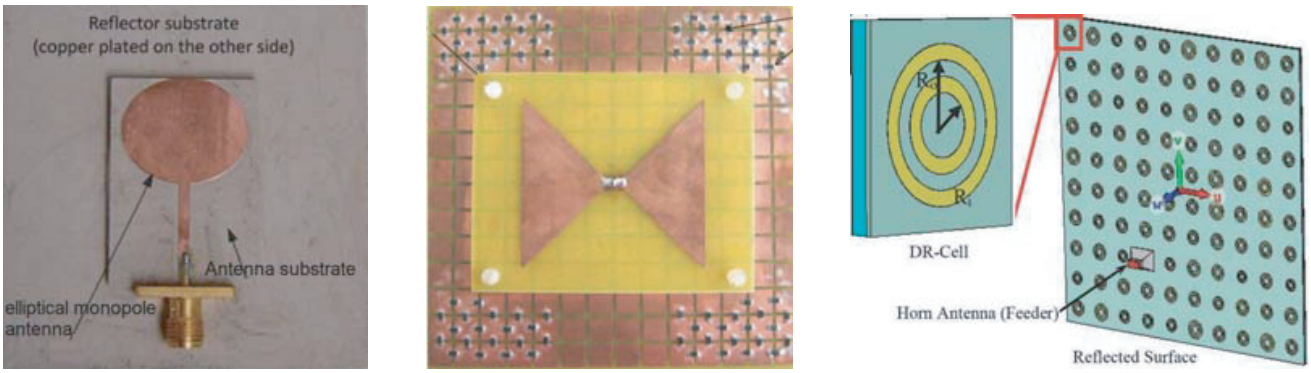

(a) (b) (c)

Figure 19. Ultrawideband planar antennas: (a) elliptical monopole antenna with reflector ($60 \times 60\,\text{mm}^2$) [56], (b) bowtie antenna with high impedance surface (HIS) [58], and (c) DR-cell and reflectarray antenna [59].

electromagnetic properties. These artificial materials are characterized by an electromagnetic bandgap (EGB) into which surface waves cannot spread [58]. Figure 19(b) shows an example of this HIS reflector. Another similar technique is presented in [59] as can been seen in Figure 19(c). Hasan et al. [59] designed a very directive reflectarray antenna (RA), which consists of two main parts: feeding part, which feeds cells of the RA on the reflection surface, and reflection surface that contains the unit-cell. The design employs Double-Ring (DR) elements as a unit-cell for the reflection surface to resonate at 2.2 GHz aiming at high penetration for human body tissues and fat. The RA reflection surface is composed of 10×10 DR cells and fed with a rectangular waveguide horn antenna as shown in Figure 19(c).

The RA achieves a pencil beam with a high directivity gain of 19.6 dBi and HPBW of 16 as shown in Figure 20(a). The radiated EM fields from the RA and horn antennas are applied to a women breast model, and the results of this study show that the RA provides much better performance than the horn antenna from the special scanning resolution, penetration depth (penetration depth in the case of RA is much larger than the penetration depth in the case of horn antenna) and the power loss distribution. Figures 20(b) and 20(c) show the penetration depth on the woman breast model of the horn antenna and the RA, respectively.

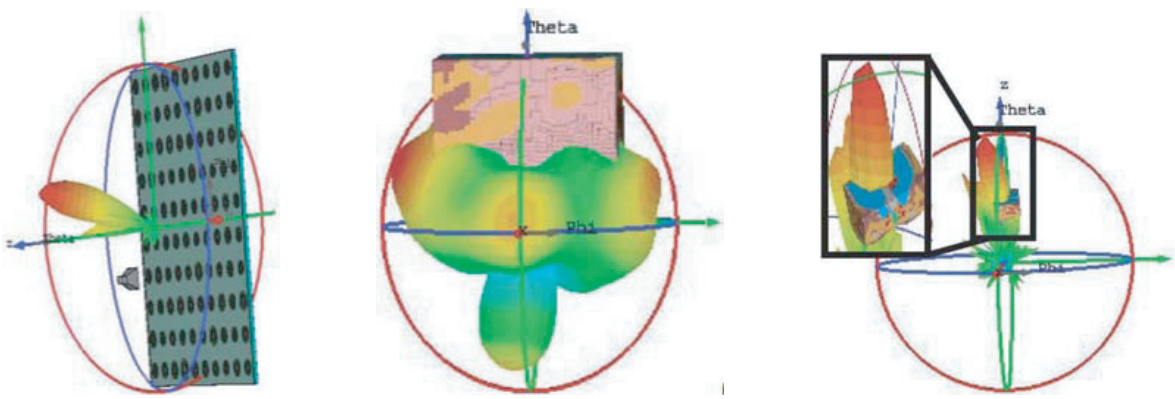

(a) (b) (c)

Figure 20. The 3D radiation pattern of RA: (a) pencil beam of RA [59], (b) penetration depth in the women breast model using a horn antenna [59], and, (c) penetration depth in the women breast model using a RA [59].

A technique used to increase the directivity is presented by Bashri et al. in [60]. The array, with 8 monopole antennas, is attached to a lossy dielectric absorber to suppress the back-lobe radiation of the monopole as can be seen in Figure 21. The outer side of the absorber is covered with aluminium tape to increase the directivity of the monopole antenna, which would increase accuracy of the imaging system [60]. The operating frequency is around 1.5 to 4 GHz to ensure enough penetration depth of the EM wave inside the human head, and the gain is improved by 2 dBi with reference to the monopole antenna without absorber [60].

Nowadays, microwave image based systems look for a proper resolution (by using broadband signals) and penetration (by using low frequency signals) as well as electromagnetic sensors to illuminate the target in small areas [61]. The latter has the purpose of having higher efficiency on the scatter map reconstruction without involving any reflection of adjacent objects to the mass of interest. That is, we can have a better permittivity changes resolution in biological tissues if the sensors are more directive and use UWB signals. However, most of the elements that make up such systems are wideband antennas of, around, 70% to 140% fractional bandwidth. To increase the bandwidth, in most antennas, it is necessary to modify its geometry, involving the modification of feeding structures and the use of coupling techniques [62]. An element that meets such requirements as a planar structure, low profile, light weight, and wide-band applications is the Vivaldi antenna [63]. In addition, it is a co-planar structure with moderate directivity, radiation endfire, and radiation patterns symmetrical in the E-H planes, easy to manufacture and economical as shown in Figure 22.

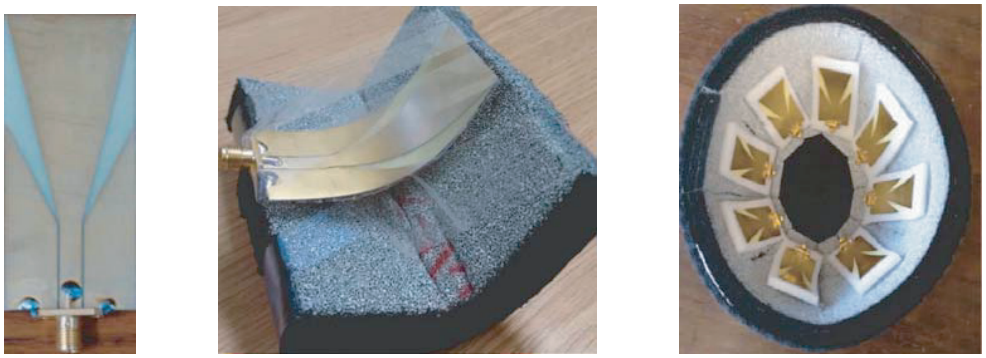

(a) (b) (c)

Figure 21. Flexible UWB monopole antennas: (a) fabricated antennas [60], (b) antenna with metal backed dielectric absorber [60], and (c) wearable microwave head imaging [60].

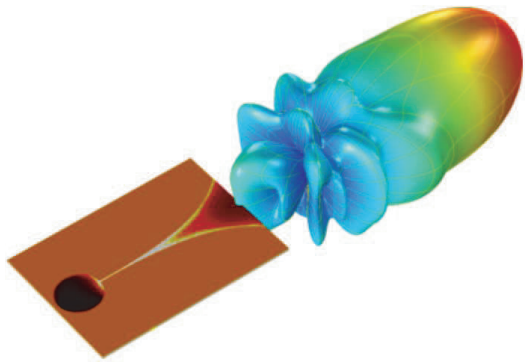

Figure 22. 3-D radiation pattern of Vivaldi antenna [64].

4. UWB VIVALDI ANTENNAS IN MICROWAVE IMAGING SYSTEMS

Vivaldi antennas belong to the tapered slot antennas (TSAs) family. Figure 23(a) shows a TSA. Wang et al. [65] present a directive antenna based on the tapered slot structure with stable radiation characteristics, in which a pair of curved slots is located near the open end of the tapered aperture

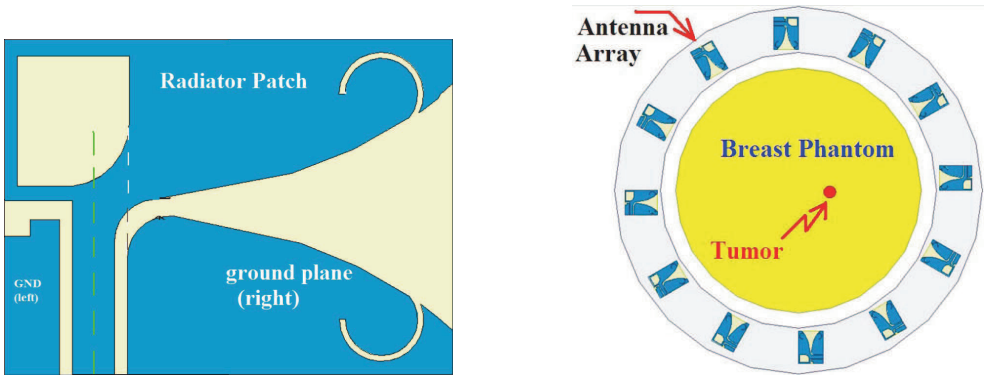

(a) (b)

Figure 23. Tapered slot antenna: (a) configuration [65], and (b) array of 12 elements integrated on a common substrate surrounding the breast [65].

to increase radiation efficiency and decrease return loss at lower frequency band. A semi-rectangular slot on the left side of the radiating patch improves the radiation pattern because this forces more surface current to flow to the right-part patch where the traveling-wave mechanism dominates the radiation [65]. The proposed antenna is used in an array of 12 elements for microwave breast imaging as shown in Figure 23(b).

Vivaldi antennas are endfire traveling wave antennas type, planar antennas whose both the current and voltage distributions can be represented by one or more traveling waves, and there exists a close relationship between the dispersion characteristics of the antenna and the radiation patterns [66]. Theoretically, a Vivaldi antenna has an infinite bandwidth [67] with its dimensions its only limit. However, it is well known that for higher frequencies, bandwidth is limited by the transition between the feeding system and slotline, while for lower frequencies, the cutoff frequency is generated by the limitation in the width of the patch or antenna taper.

An example of Vivaldi antenna is shown in Figure 24 [68], which is used in an imaging system for breast cancer detection. Zhang et al. [68] present an individual element for the breast scan as seen in Figure 24(a).

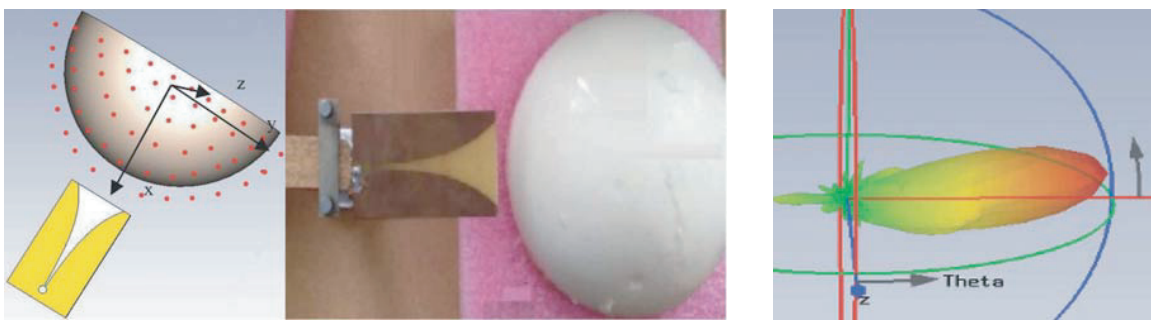

(a) (b)

Figure 24. Antenna for imaging system for the breast cancer detection: (a) scenario of measurement [68] and (b) radiation pattern of Vivaldi antenna [68].

The system can create image by using a Vivaldi antenna operating between 5 and 10 GHz, and a pencil-like radiation pattern as shown in Figure 24(b). Due to this, it turns out to be a system in which there is no mutual coupling between elements, less complex structure and simple processing, and therefore economical compared to multi-static systems [68].

They have also been used in systems for brain cancer detection as presented in [69, 70]. In this specific case, human head consists of more layers of lossy tissues than breast making it more challenging to detect the presence of cancer, thus, the antenna must have high gain to provide a sufficient penetration depth of the EM wave, and as a result, a better resolution of the image will be obtained [60]. So, very small tumours can be targeted when the body is scanned [69]. Zhang et al. suggested in [69] that there is a difference of specific absorption rate (SAR) between a healthy brain and one with a tumour, and the latter increases the SAR.

Many efforts have been dedicated to design several variants of exponential-type slot antennas (ETSAs) enhancing antenna gain and directivity. These modifications can regard the feeding structure, the geometry of exponential profile of the taper, slots modifications and the use of different dielectric materials. By modifying the feeding structure in a conventional Vivaldi antenna, as shown in Figure 24, it is possible to get an antipode configuration as shown in Figure 25(a). The tapers are separated by placing one on the front face of the dielectric and the other on the back side, achieving a higher bandwidth than a conventional one [62]. Examples of this type of antennas can be observed in [71–74]. In [71, 72], both antennas operate in UWB band frequency with total dimensions of $50 \times 50\,\text{mm}^2$ on a RT6010LM substrate ($\varepsilon_r = 10.2$) and maximum gains of 9 dB at high frequencies. However, to improve directivity of the antenna, in [73] resistive layers were incorporated with the radiating elements of the antenna on an RT4003 substrate ($\varepsilon_r = 3.38$). The gain is improved by more than 1 dB for low and high frequencies. The efficiency is more than 80% across the whole band, and the antenna maintains its UWB

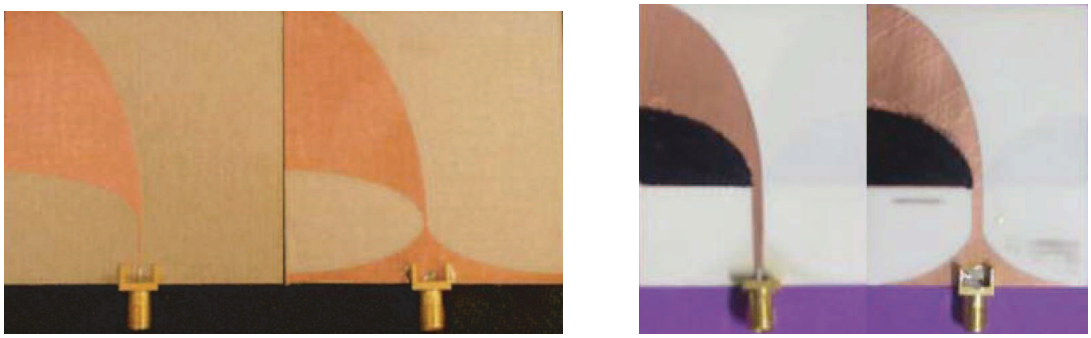

(a) (b)

Figure 25. Antipodal Vivaldi antenna: (a) fabricated AVA [72], and (b) fabricated AVA with resistive layers [73].

performance concerning return loss, even with the presence of the human body near the antenna [73].

In [74], this type of antenna is employed in a microwave system for head imaging. The system operates across a wideband frequency range from 1 GHz to 4 GHz to offer a reasonable compromise between the required head penetration of low-power microwave signals and acceptable image resolution. The system includes a semielliptical array of 16 exponentially corrugated tapered slot antenna elements with dimensions of $94 \times 110\,\text{mm}^2$ as shown in Figure 26.

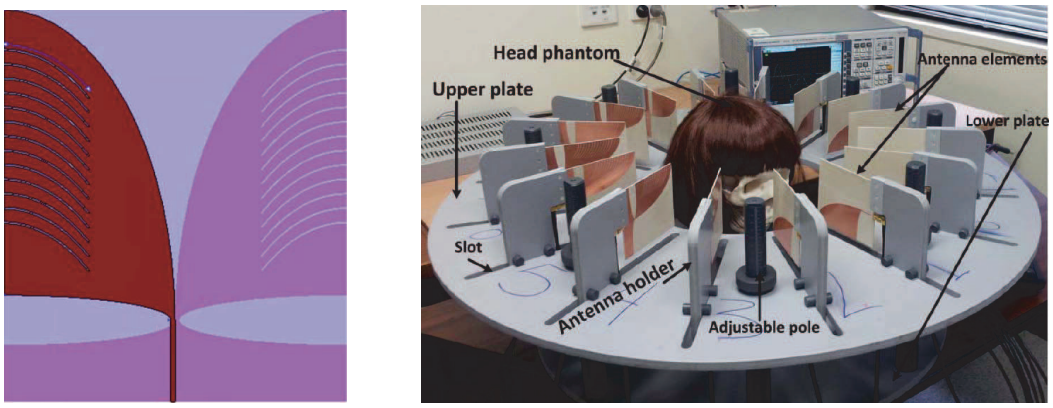

(a) (b)

Figure 26. Exponentially corrugated tapered slot antenna: (a) configuration element [74], and (b) microwave imaging system [74].

One limitation of the antipodal Vivaldi antenna is that it cannot be suitable in a phase array environment because of its very poor cross-polarization performance [75]. To solve this problem, it is necessary to balance the currents on each radiator element, doubling both the dielectric material and radiator as shown in Figure 27 [76]. The balanced antipodal Vivaldi antenna has a stripline feed, which serves the function of balanced twin line to balanced Vivaldi antenna transition, and therefore, this feeding arrangement does not limit the bandwidth as in an antipodal Vivaldi antenna, and the electric fields are no longer oblique [75]. This is achieved because the resulting field is parallel to the substrate over the entire frequency range, which results in lower cross-polarization levels and obtains higher gains when being used in antenna arrangements [75].

An arrangement of 7 antipodal balanced Vivaldi antennas is presented in [77], operating between 2.5 and 8.5 GHz as seen in Figure 28(a). Here, Yang and Mohan illuminate the breast with UWB pulses using the central element of the 7-element Vivaldi array, and the rest of the elements are used as receivers. The fidelity in the imaging system is obtained by measuring the pulse distortion radiated

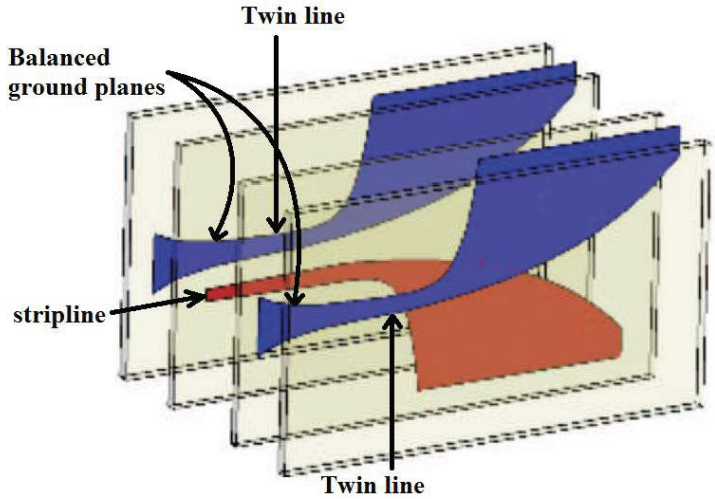

Figure 27. Balanced antipodal Vivaldi antenna (BAVA) with the 3 copper layers and the 4 dielectric layers [76].

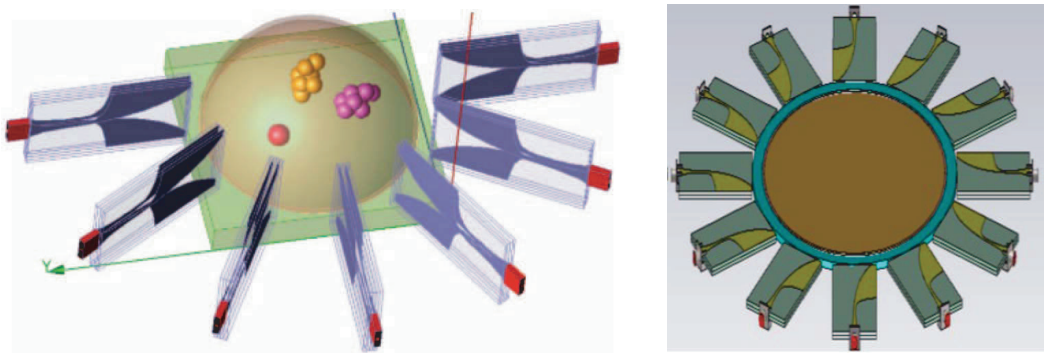

(a) (b)

Figure 28. Antennas array for systems for breast cancer detection: (a) balanced antipodal Vivaldi 7-elements array [77] and (b) balanced antipodal Vivaldi 12-elements array [78].

from the excitation pulse, thus it measures the fidelity by taking the maximum magnitude of the cross-correlation between the normalized measured response and the ideal response [77]. In this array, the results indicate that the Vivaldi antenna element does not significantly distort the signal.

Unlike the array shown in Figure 28(a), [78] presents a 12-element array covering the entire breast mass. The array shown in Figure 28(b) can operate in three different bands (0.5–1 GHz, 1.7–2 GHz, 2.8–3.1 GHz), and as in the previous array, the elements are spaced by 30. Ahsan et al. [78] conclude that the greater the number of elements constitute the array, the higher the quality is. However, even when the Vivaldi antipodal balanced antennas operate efficiently at lower frequencies (frequencies relevant for the tomography at microwaves), the endfire radiation is not reached. This is an important limitation of the present system for microwave tomography [78].

Because of its attractive features, the antipodal balanced Vivaldi antenna can be used in an imaging system as the only electromagnetic sensor, as seen in Figure 29(a). The antenna operates between 2.4 and 12 GHz by radiating 70% of the energy in the direction of the endfire as seen in Figure 29(b). The total dimension of the element is $80 \times 44\,\text{mm}^2$, and fidelity measurements indicate that the sensor meets the design requirements for its use in an adaptive radar system for sensing tissue [76].

In order to enhance the gain in the Microwave Imaging Systems, Bourqui et al. present in [79] a modification in a balanced antipodal Vivaldi antenna described in [76]. The directivity of the antenna

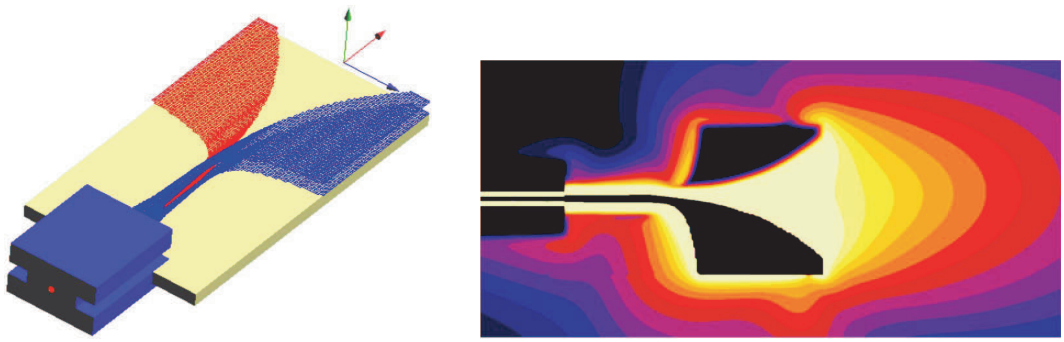

(a) (b)

Figure 29. BAVA: (a) FDTD model [76] and (b) simulated total energy flux density (EFD) in dB of the antenna [76].

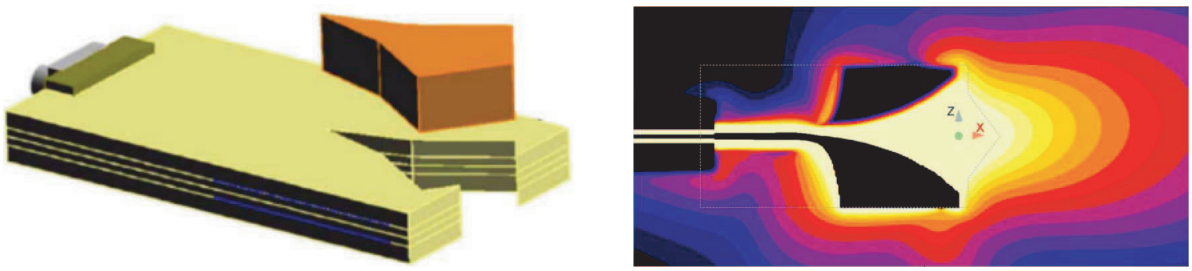

(a) (b)

Figure 30. BAVA including the higher dielectric permittivity director: (a) 3D view with the director [79] and (b) simulated total energy flux density (EFD) in dB of the antenna [79].

is remarkably improved by the inclusion of a dielectric material of higher dielectric constant at the antenna aperture which is termed "conductor", as seen in Figure 30(a). The director element has two different effects. The first is that it should act as a structure that guides the waves and directs most of the energy to the centre of the aperture. The second one is regarding the phase velocity, which should be smaller in the director structure than the rest of the substrate. The latter produces differences in the propagation velocities in the director and copper edges [79]. The material of the director is twice of the permittivity with which the antenna was constructed ($\varepsilon_r = 6$), and the S_{11} coefficient is not affected, so it operates in the same way as the antenna shown in Figure 29.

Similar to [79], in [80] a BAVA is modified for its use in microwave tomography, where the frequency range of interest is significantly lower than the UWB range down to 1 GHz. The reason for the antenna operating at this low frequency is that at higher frequencies, the depth of penetration of the electromagnetic waves is lower, directly impacting in the attenuation of the wave in the skin [19]. The dimensions are $75 \times 100\,\text{mm}^2$, and the director is twice the value of relative permittivity of the substrate, equal to 6. The director enables the BAVA to focus the radiated energy in the end-fire direction in the near-field region but only at higher frequencies, and at lower frequencies, around 1 GHz, the director has no effect as can be seen in Figure 31 [80].

Figure 32 shows an antenna that includes a lens with dielectric properties same as the antenna (Arlon AD255 $\varepsilon_r = 2.55$). The innovation is based on the elliptical shape dielectric lens which joints in front of the antennas aperture [21]. As in the previous design [80], the antenna consists of three components and two substrate layers, and two metal components serve as ground planes while the middle patch is the active conducting component [21, 80]. The elliptical shaping reduces the mismatch due to the dielectric-air interface, and the peak gain of the structure of Figure 32(b) is approximatively 12 dB [21].

In order to enhance the gain in the imaging systems, Elsherbini et al. present in [61] a technique to obtain a greater gain without using a Vivaldi antenna array. Their proposal, specifically, is based on the

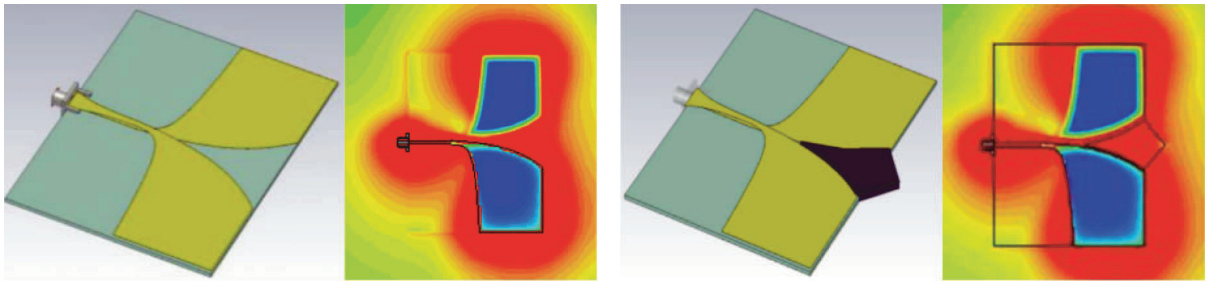

(a) (b)

Figure 31. Balanced antipodal Vivaldi antennas at 1.1 GHz: (a) BAVA without director and the near field plot [80], and (b) BAVA with director and the near field plot [80].

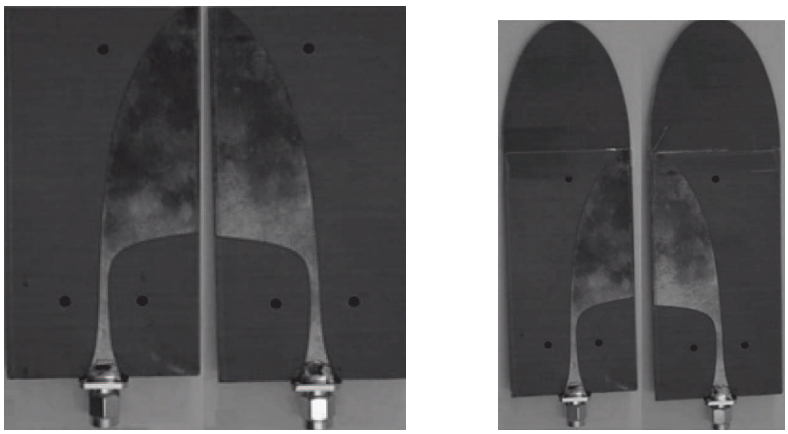

(a) (b)

Figure 32. Fabricated balanced antipodal Vivaldi antenna: (a) original ($96 \times 50\,\text{mm}^2$), and (b) with dielectric lens $146 \times 50\,\text{mm}^2$ [21].

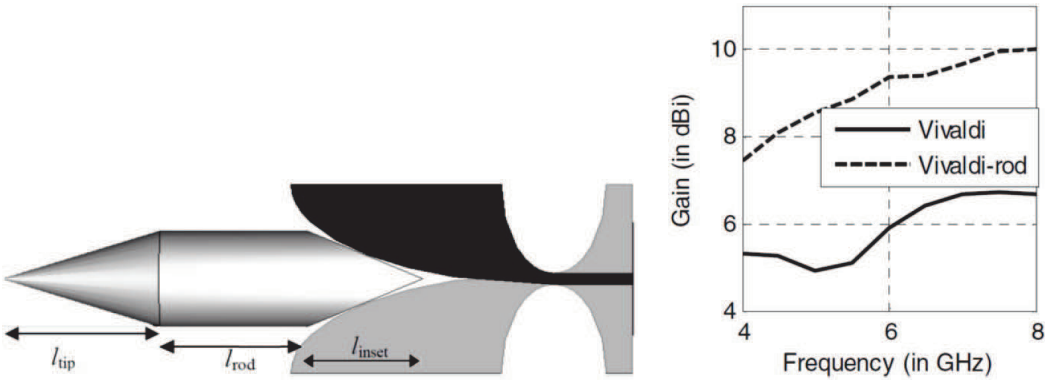

(a) (b)

Figure 33. Antipodal Vivaldi antenna with dielectric rod: (a) the Vivaldi-rod structure [61] and (b) gain vs. frequency between conventional Vivaldi antenna and antipodal Vivaldi antenna with dielectric rod [61].

addition of a dielectric rod (polystyrene) as shown in Figure 33(a), which generates symmetric radiation patterns and higher gains in a frequency range between 4 and 8 GHz. Through this technique, the gain can be increased up to 3 dB with respect to a conventional Vivaldi antenna as shown in Figure 33(b). Furthermore, phase variations against frequency are minimized. Otherwise, they will cause notable errors in localization applications [61].

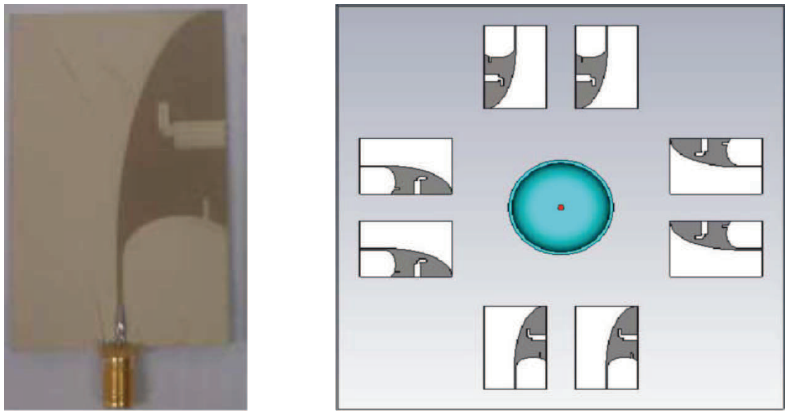

(a) (b)

Figure 34. Slot Vivaldi antenna: (a) fabricated antenna top view [81], and (b) 8-elements array surrounding the breast [81].

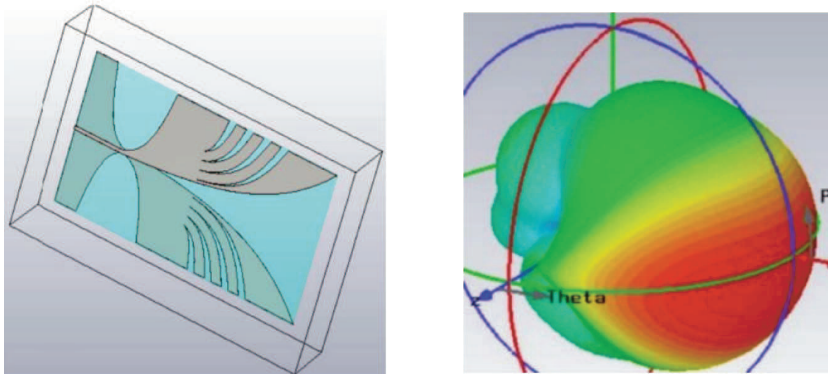

(a) (b)

Figure 35. Antipodal Vivaldi antenna for imaging systems for breast cancer detection: (a) Vivaldi antenna with exponential slots [84] and (b) 3D radiation pattern of the antenna with one exponential slot at 6 GHz [84].

As already mentioned, Vivaldi antennas are characterized by being a co-planar structure of light weight and profile, moderate directivity, symmetrical radiation patterns in the *E*-*H* planes, and good matching is observed over a wide frequency band [64], which is not enough for some UWB applications. This band limitation at high frequencies is produced by the transition between the microstrip and slotline, while at low frequencies it is generated by the limitation in the width of the patch or taper. The use of slots helps to compensate this disadvantage without having to increase the dimensions of the antenna; however, there is a certain limit so that using slots does not completely solve the problem. Bah et al. [81] implement this technique on a Vivaldi antipodal antenna as shown in Figure 34(a), and arrange 8 elements, of which 2 are transmitters and 6 receivers as shown in Figure 34(b). The array operates with a good impedance coupling between 3.1 and 10.6 GHz, with poorly directive radiation patterns and gain between 5 and 8.5 dBi, and low cross-polarization. The authors conclude that the antenna can be used in microwave imaging systems to locate, detect and even cure the tumour without interacting with the human body [81, 82].

As shown in [81], exponential-type slots are applied to an antipodal-Vivaldi antenna, as seen in Figure 35(a). This technique, better known as corrugated tapered slot antenna (TSA), provides a better coupling at lower frequencies without degrading the performance of the antenna, in addition, makes the antenna compact, improves the directivity due to its traveling wave nature, suppresses the standing waves arising in the radiator of the antenna, and enhances transmission of UWB pulses [83].

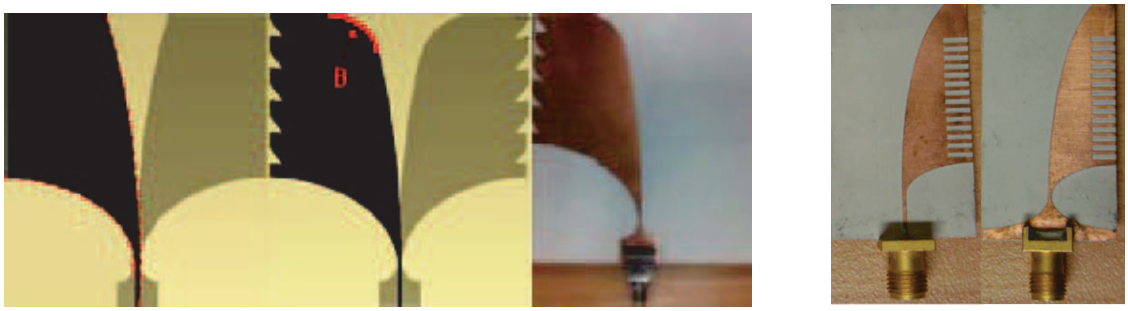

(a) (b)

Figure 36. Corrugated tapered slot antennas: (a) AVA with regular triangular-shaped slits with opening rate of the aperture [18] and (b) AVA linear slots [83].

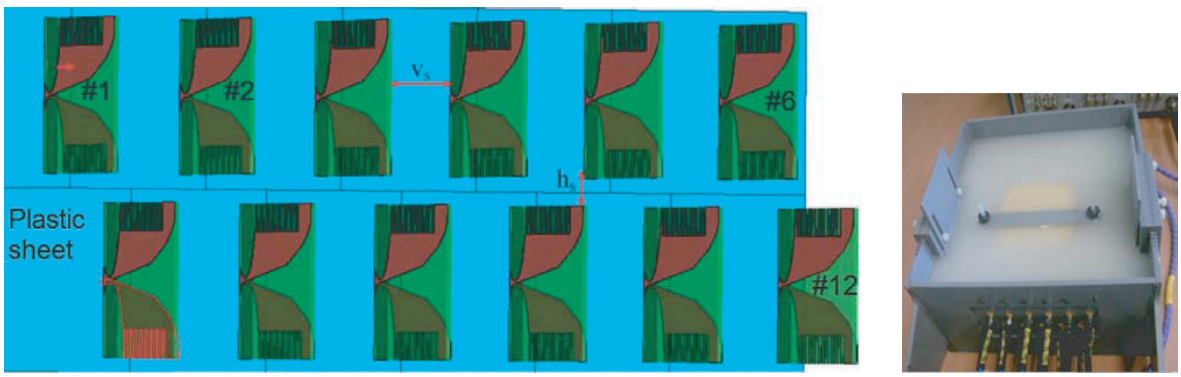

(a) (b)

Figure 37. Planar antenna array that includes 12 corrugated tapered slot elements: (a) configuration of 6×2 array [83], and (b) photograph of the breast phantom inside at the test platform with the coupling liquid [83].

The radiation patterns are stable as a function of the number of slots at higher frequencies. However, the directivity decreases as slots are inserted. For example, for a frequency of 6 GHz, the directivity for an antenna with an exponential slot is 6.7 dB while with 4 exponentials slots the directivity decays more than 0.5 dB [84].

Similar to [84], triangular and linear slots are used in [18] and [83], respectively. The AVA with regular triangular-shaped slits with opening rate of the aperture is shown in Figure 36(a), with dimensions of $96 \times 100\,\text{mm}^2$, the antenna improves the gain at low frequencies by approximately 1.5 dB compared with the conventional AVAs [85] and [86]. The AVA with linear slots is shown in Figure 36(b), and its maximum gain is approximatively 5.7 dBi (at 10 GHz). Each element is covered by a dielectric material to protect the radiating element from the adverse effects of the coupling liquid, such as metal corrosion, and to improve the matching of the antenna when being immersed in a coupling liquid [83]. The antenna shown in Figure 36(b) is used in an array that includes 12 elements for UWB biomedical microwave imaging systems as shown in Figure 37. The total size of the array is $110 \times 10 \times 10\,\text{cm}^3$.

Many efforts have been dedicated to improve the antenna parameters to get better systems. There are several antenna types reported in the literature exhibiting remarkable results. Among them high gain and wideband of approximately 8 GHz are some quite good results. The latter results have been achieved by using Vivaldi planar antennas. Besides, it has been found that the use of higher permittivity materials enhances the antenna performance, so the research of novel materials will help the cancer detection systems improvement. However, it should not be omitted that the use of substrates with higher allowances also represent greater losses due to the conductor and dielectric, which will produce a direct degradation in the efficiency of the antenna.

It is desirable to employ a single element in biomedical image detection systems since the antenna arrays show some deficiencies depending on the location of the antennas in relation to the breast. Therefore, it has been observed that the Vivaldi antenna is an interesting alternative to be used in biomedical image detection systems as an individual element.

5. CONCLUSIONS

Microwave imaging systems, as in any radioelectronic system, require transducers as medium couplers, and the reconstruction of the image in such systems will be a function of the performance of the antenna. This antenna type optimization makes building portable systems possible and therefore facilitates the operation of the equipment, reducing testing times and costs. In addition, the signals used for the reconstruction of the image are more accurate in detection of cancerous tissues in an early development stage.

Several antennas have been reported for more accuracy on detection of cancerous tissues purposes systems. The results of these research efforts are mainly focused on planarized antennas which are widely used so far. It leads to a large variety of designs and characteristics as presented in this article. However, one of the structures that stands out among others is the UWB high directive antenna due to its main features, positioning it as one of the most suitable for use in microwave imaging systems. It is possible to find that there is a wide variety of Vivaldi antennas; however, none of these prototypes present continuous bandwidths, to be specific from 1 to 10 GHz, high gain, high directivity, low profile, etc. So, it can achieve a better imaging resolution and greater EM waves penetration in biological tissues, which enables greater depth of abnormality detections.

Thus, electromagnetic sensors' optimization is critical to replace current imaging systems based on X-rays by those operating at microwave frequencies. The results are very promising so far; however, it is necessary to keep dedicating many efforts to design new microwave structures and novel antenna setup to enhance the reported results focusing on higher gain, broader bands while keeping the antenna size.

REFERENCES

1. Shin, S., *El cáncer*, https://www.aecc.es/SobreElCancer/elcancer/Paginas/Elcancer.aspx, accessed Enero, 2017.
2. Fariñas-Coronado, W., Z. Paz, G. J. Orta, and E. Rodrìguez-Denis, "Estudio del factor de disipación dieléctrica como herramienta diagnóstica," *Revista Biomdica*, Vol. 13, No. 4, 249–255, 2002.
3. Fass, L., "Imaging and cancer: A review," *Molecular Oncology*, Vol. 2, No. 2, 115–152, 2008.
4. Gallego, A. R., "Riesgos derivados de la exposición a dosis bajas de radiación ionizante," *Revista de Salud Ambiental*, Vol. 10, Nos. 1–2, 43–48, 2010.
5. Núñez, M., "Efectos biológicos de las radiaciones-dosimetra," *Escuela Universitaria de Tecnología Médica UdelaR Comité de Tecnólogos de ALASBIMN*, Montevideo, Uruguay, 2008.
6. Roldan, T., V. Aramburu, G. Leguizamon, and C. Hoffmann, "Efectos Biológicos de las radiaciónes Ionizantes," *Ciencia*, Vol. 1, No. 1, 321–330, 2003.
7. Real Gallego, A., "Efectos biológicos de las radiaciones ionizantes," *Master de Física Biomédica*, Vols. Facultad CC, Físicas-UCM, 2014.
8. Hagness, S. C., A. Taflove, and J. E. Bridges, "Two-dimensional FDTD analysis of a pulsed microwave confocal system for breast cancer detection: Fixed-focus and antenna-array sensors," *IEEE Transactions on Biomedical Engineering*, Vol. 45, No. 12, 1470–1479, 1998.
9. Hagness, S. C., A. Taflove, and J. E. Bridges, "Three-dimensional FDTD analysis of a pulsed microwave confocal system for breast cancer detection: Design of an antenna-array element," *IEEE Transactions on Antennas and Propagation*, Vol. 47, No. 5, 783–791, 1999.
10. Fear, E. C. and M. A. Stuchly, "Microwave system for breast tumor detection," *IEEE Microwave and Guided Wave Letters*, Vol. 9, No. 11, 470–472, 1999.

11. Fear, E. C. and M. A. Stuchl, "Microwave detection of breast cancer," *IEEE Transactions on Microwave Theory and Techniques*, Vol. 48, No. 11, 1854–1863, 2000.
12. Pagliari, D. J., A. Pulimeno, M. Vacca, J. A. Tobon, F. Vipiana, M. R. Casu, and L. P. Carloni, "A low-cost, fast, and accurate microwave imaging system for breast cancer detection," *IEEE Biomedical Circuits and Systems Conference (BioCAS)*, 1–4, 2015.
13. Surowiec, A. J., S. S. Stuchly, J. R. Barr, and A. A. S. A. Swarup, "Dielectric properties of breast carcinoma and the surrounding tissues," *IEEE Transactions on Biomedical Engineering*, Vol. 35, No. 4, 257–263, 1988.
14. Grzegorczyk, T. M., P. M. Meaney, P. A. Kaufman, and K. D. Paulsen, "Fast 3-D tomographic microwave imaging for breast cancer detection," *IEEE Transactions on Medical Imaging*, Vol. 31, No. 8, 1584–1592, 2012.
15. Fear, E. C., P. M. Meaney, and M. A. Stuchly, "Microwaves for breast cancer detection?," *IEEE Potentials*, Vol. 22, No. 1, 12–18, 2003.
16. Nilavalan, R., J. Leendertz, I. J. Craddock, A. Preece, and R. Benjamin, "Numerical analysis of microwave detection of breast tumours using synthetic focussing techniques," *IEEE Antennas and Propagation Society International Symposium*, Vol. 3, 2440–2443, 2004.
17. Lazebnik, M., L. McCartney, D. Popovic, C. B. Watkins, M. J. Lindstrom, J. Harter, and S. C. Hagness, "A large-scale study of the ultrawideband microwave dielectric properties of normal breast tissue obtained from reduction surgeries," *Physics in Medicine and Biology*, Vol. 52, No. 10, 2637, 2007.
18. Moosazadeh, M. and S. Kharkovsky, "Design of ultra-wideband antipodal Vivaldi antenna for microwave imaging applications," *IEEE International Conference on Ubiquitous Wireless Broadband (ICUWB)*, 1–4, 2015.
19. Ruvio, G., M. J. Ammann, M. John, R. Solimene, A. D'Alterio, and R. Pierri, "UWB breast cancer detection with numerical phantom and Vivaldi antenna," *IEEE International Conference on Ultra-Wideband (ICUWB)*, 8–11, 2011.
20. Afifi, A. I., A. B. Abdel-Rahman, A. Allam, and A. A. El-Hameed, "A compact ultra-wideband monopole antenna for breast cancer detection," *IEEE 59th International Midwest Symposium on Circuits and Systems (MWSCAS)*, 1–4, 2016.
21. Molaei, A., M. Kaboli, S. A. Mirtaheri, and M. S. Abrishamian, "Dielectric lens balanced antipodal Vivaldi antenna with low cross-polarisation for ultra-wideband applications," *IET Microwaves, Antennas & Propagation*, Vol. 8, No. 14, 1137–1142, 2014.
22. Bahrami, H., E. Porter, A. Santonelli, B. Gosselin, M. Popovic, and L. A. Rusch, "Flexible sixteen monopole antenna array for microwave breast cancer detection," *36th Annual International Conference of the IEEE Engineering in Medicine and Biology Society (EMBC)*, 3775–3778, 2014.
23. Islam, M. M., M. T. Islam, M. Samsuzzaman, M. R. I. Faruque, and N. Misran, "Microstrip line-fed fractal antenna with a high fidelity factor for UWB imaging applications," *Microwave and Optical Technology Letters*, Vol. 57, No. 11, 2580–2585, 2015.
24. Zehforoosh, Y., M. Naser-Moghadasi, S. Ra, and C. Ghobadi, "Miniature monopole fractal antenna with inscribed arrowhead cuts for UWB applications," *IEICE Electronics Express*, Vol. 9, No. 24, 1855–1860, 2012.
25. Naser-Moghadasi, M., R. A. Sadeghzadeh, T. Aribi, T. Sedghi, and B. S. Virdee, "UWB monopole microstrip antenna using fractal tree unit-cells," *Microwave and Optical Technology Letters*, Vol. 54, No. 10, 2366–2370, 2012.
26. Tripathi, S., A. Mohan, and S. Yadav, "Ultra-wideband antenna using Minkowski-like fractal geometry," *Microwave and Optical Technology Letters*, Vol. 56, No. 10, 2273–2279, 2014.
27. Abbosh, A. M., H. K. Kan, and M. E. Bialkowski, "Compact ultra-wideband planar tapered slot antenna for use in a microwave imaging system," *Microwave and Optical Technology Letters*, Vol. 48, No. 11, 2212–2216, 2006.
28. Abbosh, A. M., "Miniaturized microstrip-fed tapered-slot antenna with ultrawideband performance," *IEEE Antennas and Wireless Propagation Letters*, Vol. 8, 690–692, 2009.

29. Gibbins, D., M. Klemm, I. J. Craddock, J. A. Leendertz, A. Preece, and R. Benjamin, "A comparison of a wide-slot and a stacked patch antenna for the purpose of breast cancer detection," *IEEE Transactions on Antennas and Propagation*, Vol. 58, No. 3, 665–674, 2010.
30. Islam, M. M., M. T. Islam, M. Samsuzzaman, and M. R. I. Faruque, "A negative index metamaterial antenna for UWB microwave imaging applications," *Microwave and Optical Technology Letters*, Vol. 57, No. 6, 1352–1361, 2015.
31. Nilavalan, R., I. J. Craddock, A. Preece, J. Leendertz, and R. Benjamin, "Wideband microstrip patch antenna design for breast cancer tumour detection," *IET Microwaves, Antennas & Propagation*, Vol. 1, No. 2, 277–281, 2007.
32. Benjamin, R., I. J. Craddock, G. S. Hilton, S. Litobarski, E. Mc Cutcheon, R. Nilavalan, and G. N. Crisp, "Microwave detection of buried mines using non-contact, synthetic near-field focusing," *IEE Proceedings — Radar, Sonar and Navigation*, Vol. 148, No. 4, 233–240, 2001.
33. Nilavalan, R., A. Gbedemah, I. J. Craddock, X. Li, and S. C. Hagness, "Numerical investigation of breast tumour detection using multi-static radar," *Electronics Letters*, Vol. 39, No. 25, 1787–1789, 2003.
34. Nilavalan, R., I. J. Craddock, A. Preece, J. Leendertz, and R. Benjamin, "Breast cancer tumour detection using microwave radar techniques," *URSI EMTS Int. Symp. on Electromag. Theory*, Vol. 1, 117–119, 2004.
35. Nilavalan, R., J. Leendertz, I. J. Craddock, R. Benjamin, and A. Preece, "Breast tumour detection using a flat 16 element array," *EMC Zurich*, 2005.
36. Craddock, I. J., A. Preece, J. Leendertz, M. Klemm, R. Nilavalan, and R. Benjamin, "Development of a hemi-spherical wideband antenna array for breast cancer imaging," *First European Conference on Antennas and Propagation, EuCAP*, 1–5, 2006.
37. Klemm, M., I. J. Craddock, J. A. Leendertz, A. Preece, and R. Benjamin, "Radar-based breast cancer detection using a hemispherical antenna array — Experimental results," *IEEE Transactions on Antennas and Propagation*, Vol. 57, No. 6, 1692–1704, 2009.
38. Klemm, M., I. J. Craddock, J. Leendertz, A. W. Preece, and R. Benjamin, "Breast cancer detection using symmetrical antenna array," *The Second European Conference on Antennas and Propagation, EuCAP*, 1–5, 2007.
39. Craddock, I. J., M. Klemm, J. Leendertz, A. W. Preece, and R. Benjamin, "An improved hemispeherical antenna array design for breast imaging," *The Second European Conference on Antennas and Propagation, EuCAP*, 1–5, 2007.
40. Klemm, M., I. Craddock, J. Leendertz, A. Preece, and R. Benajmin, "Experimental and clinical results of breast cancer detection using UWB microwave radar," *IEEE Antennas and Propagation Society International Symposium, AP-S*, 1–4, 2008.
41. Gibbins, D., M. Klemm, I. Craddock, A. Preece, J. Leendertz, and R. Benjamin, "Design of a UWB wide-slot antenna and a hemispherical array for breast imaging," *3rd European Conference on Antennas and Propagation, EuCAP*, 2967–2970, 2009.
42. Sze, J.-Y. and K.-L. Wong, "Bandwidth enhancement of a microstrip-line-fed printed wide-slot antenna," *IEEE Transactions on Antennas and Propagation*, Vol. 49, No. 7, 1020–1024, 2001.
43. Klemm, M., J. A. Leendertz, D. Gibbins, I. J. Craddock, A. Preece, and R. Benjamin, "Microwave radar-based differential breast cancer imaging: Imaging in homogeneous breast phantoms and low contrast scenarios," *IEEE Transactions on Antennas and Propagation*, Vol. 58, No. 7, 2337–2344, 2010.
44. Klemm, M., I. J. Craddock, J. A. Leendertz, A. Preece, D. R. Gibbins, M. Shere, and R. Benjamin, "Clinical trials of a UWB imaging radar for breast cancer," *Proceedings of the Fourth European Conference on Antennas and Propagation (EuCAP)*, 1–4, 2010.
45. Klemm, M., D. Gibbins, J. Leendertz, T. Horseman, A. W. Preece, R. Benjamin, and I. J. Craddock, "Development and testing of a 60-element UWB conformal array for breast cancer imaging," *Proceedings of the 5th European Conference on Antennas and Propagation (EUCAP)*, 3077–3079, 2011.

46. Jalilvand, M., X. Li, L. Zwirello, and T. Zwick, "Ultra wideband compact near-field imaging system for breast cancer detection," *IET Microwaves, Antennas & Propagation*, Vol. 9, No. 10, 1009–1014, 2015.
47. Bahramiabarghouei, H., E. Porter, A. Santorelli, B. Gosselin, M. Popovic, and L. A. Rusch, "Flexible 16 antenna array for microwave breast cancer detection," *IEEE Transactions on Biomedical Engineering*, Vol. 62, No. 10, 2516–2525, 2015.
48. Porter, E., H. Bahrami, A. Santorelli, B. Gosselin, L. A. Rusch, and M. Popovic, "A wearable microwave antenna array for time-domain breast tumor screening," *IEEE Transactions on Medical Imaging*, Vol. 35, No. 6, 1501–1509, 2016.
49. Wang, F. and T. Arslan, "Inkjet-printed antenna on flexible substrate for wearable microwave imaging applications," *Antennas & Propagation Conference (LAPC)*, 1–4, Loughborough, 2016.
50. Katbay, Z., S. Sadek, R. Lababidi, A. Perennec, and M. Le Roy, "Miniature antenna for breast tumor detection," *IEEE 13th International New Circuits and Systems Conference (NEWCAS)*, 1–4, 2015.
51. Katbay, Z., S. Sadek, M. Le Roy, R. Lababidi, A. Perennec, and P. F. Dupré, "Microstrip back-cavity Hilbert fractal antenna for experimental detection of breast tumors," *IEEE Middle East Conference on Antennas and Propagation (MECAP)*, 1–4, 2016.
52. Afyf, A., L. Bellarbi, A. Errachid, and M. A. Sennouni, "Flexible microstrip CPW sloted antenna for breast cancer detection," *International Conference on Electrical and Information Technologies (ICEIT)*, 292–295, 2015.
53. Khaleel, H. R., H. M. Al-Rizzo, and A. I. Abbosh, "Design, fabrication, and testing of flexible antennas," *Advancement in Microstrip Antennas with Recent Applications*, 363–383, 2013.
54. Majid, H. A., M. K. Abd Rahim, and T. Masri, "Microstrip antenna's gain enhancement using left-handed metamaterial structure," *Progress In Electromagnetics Research M*, Vol. 8, 235–247, 2009.
55. Shrivervik, A. K., J. F. Zurcher, O. Staub, and J. R. Mosing, "PCS antenna design: The challenge of miniaturization," *IEEE Antennas and propagation Magazine*, Vol. 43, No. 4, 12–27, 2001.
56. Latif, S., D. Flores-Tapia, S. Pistorious, and L. Shafai, "A planar ultrawideband elliptical monopole antenna with reflector for breast microwave imaging," *Microwave and Optical Technology Letters*, Vol. 56, No. 4, 808–813, 2014.
57. Song, H., S. Kubota, X. Xiao, and T. Kikkawa, "Design of UWB antennas for breast cancer detection," *International Conference on Electromagnetics in Advanced Applications (ICEAA)*, 321–322, 2016.
58. Thior, A., A. C. Lepaga, and X. Begaud, "Low profile, directive and ultra wideband antenna on a high impedance surface," *3rd European Conference on Antennas and Propagation, EuCAP*, 3222–3226, 2009.
59. Hasan, K., M. El Hadidy, and H. Morsi, "Reflectarray antenna for breast cancer detection and biomedical applications," *IEEE Middle East Conference on Antennas and Propagation (MECAP)*, 1–3, 2016.
60. Bashri, M. S., T. Arslan, W. Zhou, and N. Haridas, "Wearable device for microwave head imaging," *46th European Microwave Conference (EuMC)*, 671–674, 2016.
61. Elsherbini, A., C. Zhang, S. Lin, M. Kuhn, A. Kamel, A. E. Fathy, and H. Elhennawy, "UWB antipodal vivaldi antennas with protruded dielectric rods for higher gain, symmetric patterns and minimal phase center variations," *IEEE Antennas and Propagation Society International Symposium*, 1973–1976, 2007.
62. Peyrot Solis, M. A., G. M. Galvan Tejada, and H. Jardon Aguilar, "State of the art in ultra-wideband antennas," *2nd International Conference on Electrical and Electronics Engineering*, 101–105, 2005.
63. Bai, J., S. Shi, and D. W. Prather, "Modified compact antipodal Vivaldi antenna for 4–50-GHz UWB application," *IEEE Transactions on Microwave Theory and Techniques*, Vol. 59, No. 4, 1051–1057, 2011.

64. Bhavanam, S. N. and V. Midasala, "Design of Vivaldi antenna," *Proceedings of International Conference on Innovations in Electronics and Communication Engineering (ICIECE)*, 28–34, 2014.
65. Wang, Y., A. Abbosh, and B. Henin, "Microwave breast imaging sensor using compact and directive antenna with fixed mainbeam direction," *Cairo International Biomedical Engineering Conference (CIBEC)*, 187–190, 2012.
66. Kikuta, K. and A. Hirose, "Dispersion characteristics of ultra wideband antennas and their radiation patterns," *Proceedings of URSI International Symposium on Electromagnetic Theory (EMTS)*, 462–465, 2013.
67. Gibson, P. J., "The Vivaldi aerial," *9th European IEEE Microwave Conference*, 101–105, 1979.
68. Zhang, H., T. Arslan, and B. Flynn, "A single antenna based microwave system for breast cancer detection: Experimental results," *IEEE Antennas and Propagation Conference (LAPC)*, 477–481, Loughborough, 2013.
69. Zhang, H., A. O. El-Rayis, N. Haridas, N. H. Noordin, A. T. Erdogan, and T. Arslan, "A smart antenna array for brain cancer detection," *IEEE Antennas and Propagation Conference (LAPC)*, 1–4, Loughborough, 2011.
70. Angel, J. J. and T. A. J. Mary, "Design of Vivaldi antenna for brain cancer detection," *International Conference on IEEE Electronics and Communication Systems (ICECS)*, 1–4, 2014.
71. Abbosh, A. M., H. K. Kan, and M. E. Blalkowski, "Design of compact directive ultra wideband antipodal antenna," *Microwave and Optical Technology Letters*, Vol. 48, No. 12, 2448–2450, 2006.
72. Abbosh, A. M., H. K. Kan, and M. E. Bialkowski, "Compact ultra-wideband planar tapered slot antenna for use in a microwave imaging system," *Microwave and Optical Technology Letters*, Vol. 48, No. 10, 2212–2216, 2006.
73. Abbosh, A. M., "Directive antenna for ultrawideband medical imaging systems," *International Journal of Antennas and Propagation*, Vol. 2008, 6 pages, Article ID 854012, 2008.
74. Beada'a, J. M., A. M. Abbosh, S. Mustafa, and D. Ireland, "Microwave system for head imaging," *IEEE Transactions on Instrumentation and Measurement*, Vol. 63, No. 1, 117–123, 2014.
75. Langley, J. D. S., P. S. Hall, and P. Newham, "Novel ultrawide-bandwidth Vivaldi antenna with low crosspolarisation," *Electronics Letters*, Vol. 29, No. 23, 2004–2005, 1993.
76. Bourqui, J., M. Okoniewski, and E. C. Fear, "Balanced antipodal Vivaldi antenna for breast cancer detection," *The Second European Conference on IEEE Antennas and Propagation, EuCAP*, 1–5, 2007.
77. Yang, F. and A. S. Mohan, "Microwave imaging for breast cancer detection using Vivaldi antenna array," *International Symposium on IEEE Antennas and Propagation (ISAP)*, 479–482, 2012.
78. Ahsan, S., P. Kosmas, I. Sotiriou, G. Palikaras, and E. Kallos, "Balanced antipodal Vivaldi antenna array for microwave tomography," *IEEE Conference on Antenna Measurements & Applications (CAMA)*, 1–3, 2014.
79. Bourqui, J., M. Okoniewski, and E. C. Fear, "Balanced antipodal Vivaldi antenna with dielectric director for near-field microwave imaging," *IEEE Transactions on Antennas and Propagation*, Vol. 58, No. 7, 2318–2326, 2010.
80. Ahsan, S., B. Yeboah-Akowuah, P. Kosmas, H. C. Garcia, G. Palikaras, and E. Kallos, "Balanced antipodal vivaldi antenna for microwave tomography," *EAI 4th International Conference on IEEE Wireless Mobile Communication and Healthcare (Mobihealth)*, 316–319, 2014.
81. Bah, M. H., J. Hong, D. A. Jamro, J. J. Liang, and E. A. Kponou, "Vivaldi antenna and breast phantom design for breast cancer imaging," *7th International Conference on IEEE Biomedical Engineering and Informatics (BMEI)*, 90–93, 2014.
82. Bah, M. H., J. S. Hong, and D. A. Jamro, "UWB antenna design and implementation for microwave medical imaging applications," *IEEE International Conference on Communication Software and Networks (ICCSN)*, 151–155, 2015.
83. Mohammed, B. A. J., A. M. Abbosh, and P. Sharpe, "Planar array of corrugated tapered slot antennas for ultrawideband biomedical microwave imaging system," *International Journal of RF and Microwave Computer-Aided Engineering*, Vol. 23, No. 1, 59–66, 2013.

84. Kanjaa, M., O. E. Mrabet, M. Khalladi, and M. Essaaidi, "Exponentially tapered antipodal Vivaldi antenna for breast cancer detection," *IEEE 15th Mediterranean Microwave Symposium (MMS)*, 1–3, 2015.
85. Ba, H. C., H. Shirai, and C. D. Ngoc, "Analysis and design of antipodal Vivaldi antenna for UWB applications," *IEEE Fifth International Conference on Communications and Electronics (ICCE)*, 391–394, 2014.
86. Cao, Y., J. Lei, Y. Wei, and L. Zhu, "A compact BAVA design with corrugated edge," *3rd Asia-Pacific Conference on Antennas and Propagation (APCAP)*, 259–262, 2014.